Chemo-responsive, self-oscillating gels that undergo biomimetic communication

Citation: Kuksenok, Olga, Pratyush Dayal, Amitabh Bhattacharya, Victor V. Yashin, Debabrata Deb, Irene C. Chen, Krystyn J. Van Vliet, and Anna C. Balazs. "Chemo-Responsive, Self-Oscillating Gels That Undergo Biomimetic Communication." Chemical Society Reviews 42, no. 17 (2013): 7257.

As Published: http://dx.doi.org/10.1039/c3cs35497k

Publisher: Royal Society of Chemistry, The

Persistent URL: http://hdl.handle.net/1721.1/93126

Version: Author's final manuscript: final author's manuscript post peer review, without publisher's formatting or copy editing

Chem Soc Rev

RSC Publishing

REVIEW ARTICLE

View Article Online
View Journal

Chemo-responsive, self-oscillating gels that undergo biomimetic communication

Cite this: DOI: 10.1039/c3cs35497k

Olga Kuksenok,[a] Pratyush Dayal,[b] Amitabh Bhattacharya,[c] Victor V. Yashin,[a] Debabrata Deb,[a] Irene C. Chen,[d] Krystyn J. Van Vliet[e] and Anna C. Balazs*[a]

Species ranging from single-cell organisms to social insects can undergo auto-chemotaxis, where the entities move towards a chemo-attractant that they themselves emit. Polymer gels undergoing the self-oscillating Belousov–Zhabotinsky (BZ) reaction exhibit autonomous, periodic pulsations, which produce chemical species collectively referred to as the activator. The diffusion of this activator into the surrounding solution affects the dynamic behavior of neighboring BZ gels and hence, the BZ gels not only emit, but also respond to self-generated chemical gradients. This review describes recent experimental and computational studies that reveal how this biomimetic behavior effectively allows neighboring BZ gels to undergo cooperative, self-propelled motion. These distinctive properties of the BZ gels provide a route for creating reconfigurable materials that autonomously communicate with neighboring units and thereby actively participate in constructing the desired structures.

Received 3rd December 2012

DOI: 10.1039/c3cs35497k

www.rsc.org/csr

1. Introduction

One of the hallmarks of biological species is the ability to communicate and, through this communication, achieve a cooperative action. Higher-level organisms can use verbal communication to transmit a message and thereby prompt collective behavior within a group. More primitive species, such as the cellular slime mold, transmit messages through a chemical signal. In particular, individual slime mold cells release a signaling molecule known as cAMP (cyclic adenosine monophosphate) that is sensed by the other cells, which then also produce cAMP.[1] Due to their ability to both transmit and sense this molecule, groups of slime mold cells undergo collective motion, traveling toward the highest concentration of cAMP. In this manner, the species can associate into larger, multi-cellular units. Recall that chemotaxis refers to the motion of organisms in response to local chemical gradients. The behavior exhibited by the slime molds is a form of auto-chemotaxis since the organisms produce the local chemical variations that promote their motion.

One of the challenges for materials science is to create synthetic systems that could mimic such primitive biological communication. In effect, it would be highly advantageous to design responsive units that could undergo auto-chemotaxis so that individual building blocks would signal each other to gather and self-organize into larger-scale structures. Such synthetic systems would need to exhibit strong coupling between chemical and mechanical behavior.

In this review, we describe the behavior of responsive gels that exhibit a distinct form of chemomechanical communication, whereby individual gel pieces both send and receive a chemical signal that causes the gels to undergo local undulations. This signaling mechanism can also drive the gels to undergo global motion. In the latter cases, the systems exhibit a form of auto-chemotaxis since they move along self-generated chemical gradients. We discuss previous findings that highlight these forms of chemo-mechanical communication among multiple gel pieces and point to very recent work[2,3] that reveals that these signaling gels can cooperatively self-organize into macroscopic structures.

The specific class of gels that exhibit this remarkable form of communication are known as "BZ gels"[4,5] because they are undergoing the Belousov–Zhabotinsky (BZ) reaction.[6,7] The BZ reaction is one of the cornerstones of the field of non-linear chemical dynamics. The reaction involves a metal catalyst (typically ruthenium, cerium or ferroin) that is driven to undergo a periodic reduction and oxidation by the combination

[a] Chemical Engineering Department, University of Pittsburgh, Pittsburgh, PA, 15261, USA. E-mail: balazs@pitt.edu
[b] Chemical Engineering Department, Indian Institute of Technology, Gandhinagar, India
[c] Mechanical Engineering Department, Indian Institute of Technology, Bombay, Powai, Maharashtra, 400076, India
[d] Department of Chemical Engineering, Massachusetts Institute of Technology, Cambridge, MA 02139, USA
[e] Department of Materials Science and Engineering and Department of Biological Engineering, Massachusetts Institute of Technology, Cambridge, MA 02139, USA

of reagents in the surrounding solution. These periodic oscillations can be readily visualized by the changes in color of the metal catalyst from the reduced to the oxidized states.[6,7] In the late 1990s, Yoshida *et al.*[4] anchored the BZ catalyst (in that case, Ru) to the backbones of the polymer chains within a gel formed from *N*-isopropylacrylamide (NIPAAm). The rhythmic reduction–oxidation of the Ru altered the characteristics of the solution with respect to the solvation of the gel. Namely, with the catalyst in the reduced state (Ru^{+2}), the solution provided a less hydrating environment and the gel became relatively collapsed; in the oxidized state (Ru^{+3}), the fluid yielded a more hydrating environment, and the gel became relatively swollen. Hence, due to the rhythmic redox reaction, the BZ gels exhibited a periodic swelling and deswelling, along with a concurrent change in the gel color from an orange to a green hue. Remarkably, no external stimuli are needed to induce the gel's regular pulsations, which are driven purely by the combination of reagents in the solution and the anchored catalyst within the gel. Hence, in a Petri dish, an isolated BZ gel sample is seen to pulsate like a beating heart.[4]

The BZ gels[4,5,8,9] are truly unique: to date, there are no other gels that oscillate in the absence of external stimuli. Notably, there are various examples of polymer gels that can be driven to pulsate through a periodic change in the local environment, which is accomplished through the use of a continuously stirred tank reactor or controlled variations in external cues.[10–17] The BZ gels, however, are the only gel system that can swell and deswell autonomously, with these mechanical oscillations being driven by the chemical oscillations of the BZ reaction. In fact, millimeter sized pieces of the BZ gels can pulsate autonomously for hours.[18,19] Moreover, these gels can be "recycled" by simply replenishing the consumed solutes, as demonstrated by Chen and Van Vliet *et al.*[20] In the latter study, the researchers showed[20] that recycled samples displayed the same pattern formation and period of oscillation as freshly prepared gels.

To date, the NIPAAm-based BZ gels[4,5,8,9,20,21] are the most analyzed and understood self-oscillating gels; there have, however, been a number of recent advances in utilizing different polymer networks to design these active materials. Recently, Vaia *et al.* fabricated BZ gels based on bio-derived polypeptide gelatin;[22] these gels can be post-functionalized with Ru catalyst, allowing a variety of heterogeneous patterns to be fabricated.

It is worth noting that while the NIPAAm-based and gelatin-based BZ gels swell in response to the oxidation of the metal ion catalyst, there are examples of BZ gels that show the opposite effect: namely, they deswell during the oxidation cycle of the BZ reaction. The latter effect was observed by Konotop *et al.* in composite gels based on polyacrylamide (PAAm) and silica gel, and gels of poly(acrylamide-*co*-acrylate).[23,24] Most recently, Nuzzo *et al.* synthesized a novel methacrylate modified ruthenium catalyst; this BZ reaction catalyst can be copolymerized with acrylamide units, which in turn can be driven to undergo a rapid polymerization *via* UV exposure. The resulting PAAm BZ gels are robust and exhibit relatively fast oscillations at moderate acid concentration.[25] The observed changes in volume for all the above PAAm-based BZ gels were attributed[23–25] to the formation of additional complexes between the negatively charged polymer and the oxidized catalyst. When formed, the latter complexes act as additional physical cross-links in the polymer network, and hence, lead to a decrease in the degree of swelling. These additional cross-links are reversible; they break when the catalyst is in the reduced state so that the gel re-swells back to its original size.[23–25] While these newly synthesized BZ gel systems hold great promise, in this review, we focus on the more studied NIPAAm-based BZ gels.

The self-oscillating behavior of the BZ gels makes them ideal materials for designing biomimetic systems that can exhibit autonomous functionality. Furthermore, the rhythmic changes in the volume of the gel (that occur as the network swells and deswells) can be harnessed to perform mechanical work. Taking advantage of these attributes, Yoshida *et al.* have fabricated a millimeter-sized BZ gel "worm" that "inches" along a surface in a self-sustained manner as it swells and deswells against grooves in that surface.[26,27] The latter studies pave the way for creating small-scale robots that perform useful work.

An important challenge in the design of small-scale "soft robots," or machines made of mechanically compliant materials such as polymers, is to establish means for the individual units to collaborate in performing a well-defined task. For example, dynamic reconfiguration among such robots could be enabled if the components could mimic the mode of communication exhibited by the slime molds described above. In this review, we describe examples of BZ gels that show some salient features of this mode of communication. We note that while researchers have developed a range of nano- and microscopic self-propelled particles,[28] few of these exhibit auto-chemotaxis,[29] and even fewer[30] use this mechanism to self-organize into large-scale structures. Research on synthetic auto-chemotaxing particles is still in its infancy, but recent advances[2,3] point to promising efforts in the creation of mechanically compliant materials that appear to communicate and effectively collaborate. Separate advances in automated responses for self-healing polymeric structures[31,32] and actuating structures[33] have achieved impressive macroscopic motion with nonfunctional polymers, which may eventually be augmented by use of functional, auto-chemotactic materials. Thus, these advances in responsive gels can pave the way for the design of the next generation of responsive, interactive "soft robots."

Below, we first provide background on the BZ gels and the principal chemical reactions occurring within the system. Subsequently, we describe scenarios that involve solution-mediated signaling interactions among isolated, physically fixed pieces of chemo-responsive BZ gels. We then discuss cases for which this signaling leads to collective motion of the communicating gels. Some guidelines for creating such communicating BZ gels have emerged from theoretical and computational modeling. Hence, below, we also provide a brief description of the methods that have been used to model these communicating systems.

2. Fundamentals of BZ gels

As noted above, the only known responsive polymer gels that exhibit autonomous oscillations in volume are those involved in the Belousov–Zhabotinsky (BZ) reaction. The original BZ

reaction was discovered serendipitously in the 1950s, and involved reagents in a fluid rather than a gel. The BZ reaction provides a classic example of systems that operate far from equilibrium.[6,7] Roughly forty years after the initial discovery, chemically neutral, non-responsive polymer gels were used as a medium for the BZ reaction in order to suppress hydrodynamic effects.[34] These non-responsive gels did not exhibit chemo-mechanical oscillations; this is, the polymer network did not undergo volumetric changes (swelling or deswelling) in response to the BZ reaction. It was only in 1996 that Yoshida *et al.* fabricated the first BZ reaction to take place in a responsive gel.[4] In that pioneering study, the ruthenium tris(2,2′-bipyridine) complex, $Ru(bpy)_3$, which is known to be a catalyst for the BZ reaction, was incorporated as a pendent group on cross-linked polymer chains of NIPAAm. The polymer network with the attached metal-ion catalyst was swollen in an aqueous solution of the BZ reagents: $NaBrO_3$, HNO_3, and malonic acid. The ensuing BZ reaction generated a wave of swelling and de-swelling that propagated along the length of the BZ gel. Notably, the cause for the oscillations is purely *internal*; that is, all the necessary ingredients are present only within the swollen gel. The reagents in the surrounding solution provide the "fuel" that sustains the oscillatory BZ reaction of the sample.

The swelling of the NIPAAm gel during the oxidation stage of the BZ reaction is attributed primarily to the change in the hydrophilic–hydrophobic properties of the polymer chains, *i.e.*, in the affinity of the polymer to water.[4,18] Inclusion of the $Ru(bpy)_3$ complex affects the degree of swelling of the gel to an extent that depends on the electric charge of the metal ion. Oxidation of the catalyst has a hydrating effect, and the gel swells. This hydration–dehydration mechanism of coupling between the chemical and mechanical degrees of freedom was proposed in ref. 4, and then analyzed thoroughly in ref. 18 with regard to the contribution of the polyelectrolyte effects on the NIPAAm gel swelling. Since the BZ reaction takes place in water in an acidic environment, variations of the metal ion electric charge in the course of the redox processes change the distribution of ions in the aqueous component of the gel. Hence, the degree of gel swelling is affected by the variations in the osmotic pressure of the dissolved ionic species, *i.e.*, the Donnan osmotic pressure.[35,36] In ref. 18, the oscillating force generated by cylindrical samples of BZ gels of different thickness was measured. The Donnan osmotic pressure at given degrees of swelling and catalyst oxidation was estimated theoretically based on the Flory–Huggins theory.[35] It was shown that in a thin oscillating cylinder, in which the time to achieve a quasi-equilibrium swelling and deswelling is shorter than the period of oscillation, the tensile stress variation is much higher than the amount that can be generated by the Donnan osmotic pressure. An increase in the sample diameter led to a significant decrease in the amplitude of the tensile stress oscillations, whereas the estimated variations in the Donnan pressure did not exhibit a considerable change. Therefore, it was concluded that the hydrating effect of the oxidized catalyst is responsible for the chemical to mechanical energy transduction in the NIPAAm-based BZ gels.[18]

Below, we discuss the specific chemical reactions that occur within a chemo-responsive gel undergoing the BZ reaction. We also outline the models that were used to describe these reactions and thus, create an approach for isolating factors that affect the reaction kinetics, and ultimately, the chemomechanical response of the gel to these chemical variations. The following section highlights the fact that while there are dozens of species involved in the reaction, the fundamental behavior of the both the solution and gel systems can be expressed in terms of two variables: u, the concentration of the "activator" for the reaction, and v, the concentration of the oxidized catalyst. As we show further below, it is the local concentrations of u that allow multiple gel pieces to communicate.

2.1 Kinetics of the BZ reaction in gels

The following reaction schemes apply to a cross-linked polymer network of poly(*N*-isopropylacrylamide) (NIPAAm) in which the catalyst ruthenium tris(2,2′-bipyridine) ($Ru(bpy)_3$) is anchored onto the chains.[4,5,8,37–40] This polymer network is swollen in an aqueous solution of sodium bromate ($NaBrO_3$), nitric acid (HNO_3), and malonic acid (MA); MA acts as an organic substrate for the BZ reaction. The kinetics of the BZ reaction involves two dozen reactive species and tens of chemical reactions. The main features of this reaction can be described successfully by the reaction mechanism proposed in 1972 by Field, Koros, and Noyes.[41] Within the framework of the Field–Koros–Noyes mechanism (FKN), the BZ reaction is reduced to the following three basic processes:[41–44]

$$BrO_3^- + 2Br^- + 3H^+ \rightarrow 3HOBr$$

$$BrO_3^- + HBrO_2 + 2M_{red} + 3H^+ \rightarrow 2HBrO_2 + 2M_{ox} + H_2O$$

$$2M_{ox} + MA + BrMA \rightarrow fBr^- + 2M_{red} + \text{other products}$$

The stoichiometric factor f represents the number of bromide ions produced as two oxidized metal ions (M_{ox}) are reduced (M_{red}). In the reacting polymer gels,[4,5,8,37–40] $M_{ox} = Ru(bpy)_3^{3+}$ and $M_{red} = Ru(bpy)_3^{2+}$. As noted above, the cyclic change of the electric charge on the ruthenium ion causes the periodic swelling–deswelling of the gel in the course of the BZ reaction. The gel swelling takes place when the metal ion is in the oxidized state.

The essential features of the FKN mechanism can be captured by the Oregonator model proposed by Field and Noyes in 1974.[42] Within this model, the BZ reaction is described in terms of three variables and the sequence of five chemical reactions;[41–44] herein, we use the following Tyson and Fife formulation of the Oregonator model:[45]

$$A + Y \xrightarrow{k_1 H^2} X + P$$

$$X + Y \xrightarrow{k_2 H} 2P$$

$$A + X \xrightarrow{k_3 H} 2X + 2Z$$

$$X + X \xrightarrow{k_4} A + P$$

$$B + Z \xrightarrow{k_5} \frac{1}{2} f Y$$

where A = [BrO_3^-], B = [all oxidizable organic species], H = [H^+], P = [HOBr], X = [$HBrO_2$], Y = [Br^-], and Z = [M_{ox}]. The stoichiometric factor f is considered as a model parameter. The Oregonator model treats the concentrations of the major reactants A, B, and P, as well as the concentration of the hydrogen ions H, as constants. The reaction rate equations for the species X, Y, and Z are as follows:[45,46]

$$dX/dt = k_1H^2AY - k_2HXY + k_3HAX - 2k_4X^2 \quad (1)$$

$$dY/dt = -k_1H^2AY - k_2HXY + \frac{1}{2}fk_5BZ \quad (2)$$

$$dZ/dt = 2k_3HAX - k_5BZ \quad (3)$$

In a swollen polymer gel, the polymer network with the attached metal ion catalyst occupies a volume fraction ϕ. The rest of the BZ reagents are dissolved in solvent (of volume fraction $1 - \phi$). The variable concentrations X, Y, and Z are defined with respect to the total volume of the system. In contrast, it is more convenient to define the concentrations of the reactants A, B, and H with respect to the volume of the solvent; in accordance with the original Oregonator model, we assume the concentrations of the latter reactants to be constant. Re-calculation of A, B, and H relative to the total volume is achieved through multiplication by the factor $(1 - \phi)$. As a result, the following substitutions should be made in the right-hand-sides of the reaction rate equations, eqn (1)–(3):

$$k_1H^2A \rightarrow k_1(1-\phi)^3H^2A$$

$$k_2H \rightarrow k_2(1-\phi)H$$

$$k_3HA \rightarrow k_3(1-\phi)^2HA$$

$$k_5B \rightarrow k_5(1-\phi)B$$

Thus, the polymer is assumed to act like a chemically neutral diluent, which affects the reaction rates only by changing the concentrations A, H, and B. In general, the stoichiometric factor f might also depend of the volume fraction ϕ. It is, however, taken to be constant for simplicity.

The concentration variable Y is known to change in time much faster than X and Z.[45,46] Consequently, the variable Y can be excluded from the reaction rate equations by employing the steady-state approximation $dY/dt \approx 0$.[45,46] The remaining two reaction rate equations can be conveniently written in the dimensionless form after the dimensionless concentration variables $u = X/X_0$ and $v = Z/Z_0$ are introduced utilizing the parameterization given by Tyson:[45,46] $X_0 = \frac{k_3HA}{2k_4}$, $Z_0 = \frac{(k_3HA)^2}{k_4k_5B}$. The dimensionless time variable t = time/T_0 is defined using the time scale $T_0 = (k_3HA)^{-1}$. The resulting dimensionless reaction rate equations have following form:

$$\frac{du}{dt} = F(u, v, \phi) \quad (4)$$

$$\frac{dv}{dt} = \varepsilon G(u, v, \phi) \quad (5)$$

where the reaction rate functions F and G from the Oregonator model derived by Tyson and Fife[45] are now modified to take into account the polymer volume fraction:[47]

$$F(u, v, \phi) = (1-\phi)^2u - u^2 - (1-\phi)fv\frac{u - q(1-\phi)^2}{u + q(1-\phi)^2} \quad (6)$$

$$G(u, v, \phi) = (1-\phi)^2u - (1-\phi)v \quad (7)$$

The dimensionless parameters ε and q have the same definitions as in the original Oregonator model,[45] namely: $\varepsilon = \frac{k_5B}{k_3HA}$, $q = \frac{2k_1k_4}{k_2k_3}$.

As can be seen from eqn (6) and (7), the Oregonator model specifies the kinetics of the BZ reaction through three parameters, namely q, ε, and f. The parameter q is a dimensionless combination of only the reaction rate constants, so it remains unchanged with variations in chemical composition at a constant temperature. In contrast, the Oregonator parameters ε and f are sensitive to the chemical composition of the BZ substrate, and other experimental conditions. The parameter ε is the ratio between two reaction rates: one reaction rate is for the reduction of the metal ion catalyst during the oxidation of the organic substrate and the other is for oxidation of the catalyst mediated by the BZ reactant u. Typically, oxidation of the BZ catalyst is faster than its reduction, so $\varepsilon < 1$. The stoichiometric parameter f specifies the production of the bromide ion, which inhibits the catalytic process. Thus, the value of f effectively controls the concentration of oxidized catalyst within the system in the steady state and affects the amplitude of the oscillations in the oscillatory state.[43] It is common practice in modeling the BZ reaction to keep the value of q fixed, and consider the values of ε and f as free model parameters, which control the reaction regime.[43,46]

The modified Oregonator model, eqn (6) and (7), describes the kinetics of the BZ reaction in terms of the dimensionless concentrations of the oxidized catalyst, v, and the key reaction intermediate (the activator) u; the reaction rates explicitly depend on the volume fraction of polymer, ϕ. The spatial and temporal variations of ϕ in the course of the swelling and deswelling of the gel affect the local chemical kinetics. Moreover, the BZ reaction itself induces a re-distribution of solvent within the swollen chemo-responsive hydrogel. In the next section, we consider a theoretical model that couples the chemical reaction to the dynamics of the responsive polymer gel.

2.2 Dynamics of the BZ gels

Building on the above modified Oregonator model, Balazs *et al.* derived a set of equations that describe the elastodynamics and reaction–diffusion processes occurring within the BZ gels.[48,49] They then developed a lattice-based approach, the gel lattice spring model (gLSM),[48–50] which allows us to numerically solve these governing equations in a computationally efficient manner. Furthermore, these researchers also modified the model to account for the photosensitivity of the BZ gels.[51,52]

The gLSM yielded qualitative agreement between the findings from computational studies and various experimental results. For example, in agreement with experiments, the results from this model revealed the in-phase synchronization of the chemical and mechanical oscillations for relatively small-sized samples[38,49] and a decrease of the oscillation period with an increase in the concentration of malonic acid.[5,49] Additionally, the shape- and size-dependent pattern formation observed in these gLSM simulations showed qualitative agreement with experimental studies.[20] Such simulations were also useful in explaining how gradients in crosslink density could drive long, thin BZ gels to both oscillate and bend, and thereby undergo concerted motion.[53]

Recently, we modified the gLSM approach to model patches of BZ gels that are embedded within a neutral, non-responsive gel and through this model, could successfully capture the synchronization between circular BZ gel patches[54] that encompassed different concentrations of Ru catalyst. Most recently, we further modified our gLSM model to capture the behavior of novel PAAm-based self-oscillating BZ gels, in which the oxidation of the catalysts leads to a deswelling of the sample due to the formation of additional reversible cross-links.[25] Hence, the gLSM[55,56] has proven to be a powerful approach for predicting the behavior of these self-oscillating gels.

The kinetics of the gels undergoing the photosensitive BZ reaction is described by a modified version[48] of the two-variable Oregonator model[45,46] that explicitly takes into account the polymer volume fraction, ϕ. The governing equations for this system are:[48,49]

$$\frac{\partial \phi}{\partial t} = -\nabla \cdot (\phi \boldsymbol{v}^{(p)}) \tag{8}$$

$$\frac{\partial v}{\partial t} = -\nabla \cdot (v \boldsymbol{v}^{(p)}) + \varepsilon G(u, v, \phi) \tag{9}$$

$$\frac{\partial u}{\partial t} = -\nabla \cdot (u \boldsymbol{v}^{(s)}) - \nabla \cdot \boldsymbol{j}^{(u)} + F(u, v, \phi) \tag{10}$$

Here, v and u are the respective dimensionless concentrations of the oxidized catalyst and activator; $\boldsymbol{v}^{(p)}$ and $\boldsymbol{v}^{(s)}$ are the respective velocities of the polymer network and solvent. The dimensionless diffusive flux of the solvent $\boldsymbol{j}^{(u)}$ through the gel in eqn (10) is calculated as:[48] $\boldsymbol{j}^{(u)} = -(1 - \phi)\nabla(u(1 - \phi)^{-1})$. The expression for $G(u, v, \phi)$ in eqn (9) is given in eqn (7) and the term $F(u, v, \phi)$ in eqn (10) was modified with respect to the expression in eqn (6) to account for the photosensitivity of the BZ and is written as:

$$F(u, v, \phi) = (1 - \phi)^2 u - u^2 - (1 - \phi)[fv + \Phi]\frac{u - q(1 - \phi)^2}{u + q(1 - \phi)^2} \tag{11}$$

As noted in Section 2.1, the parameters q, f and ε in the above equations have the same meaning as in the original Oregonator model.[45] The dimensionless variable Φ (see eqn (11)) was introduced into the Oregonator model by Krug *et al.* to account for the effect of light on the reaction kinetics.[57] In the absence of the polymer gel (*i.e.*, in the BZ solution), this two-variable, photosensitive Oregonator model has been used to successfully explain the observed experimental phenomena in a number of studies.[58–61] Within this model, Φ specifically accounts for the additional production of bromide ions that are due to illumination by light of a particular wavelength and Φ is assumed to be proportional to the light intensity.[57] The above approach allows us to reproduce the experimentally observed suppression of oscillations within BZ gels by visible light.[62] By setting $\Phi = 0$ in eqn (11), we recover our previous model for BZ gels in the absence of light.[48,49]

We assume the dynamics of the polymer network to be purely inertialess,[63] so that the forces acting on the deformed gel are balanced by the frictional drag due to the motion of the solvent. Hence, the corresponding force balance equation can be written as:[48]

$$\nabla \cdot \hat{\boldsymbol{\sigma}} = v_0 T^{-1} D_u \zeta(\phi)\left(\boldsymbol{v}^{(p)} - \boldsymbol{v}^{(s)}\right). \tag{12}$$

Here, $\hat{\boldsymbol{\sigma}}$ is the dimensionless stress tensor measured in units of ${v_0}^{-1}T$, where v_0 is the volume of a monomeric unit and T is temperature in energy units; $\zeta(\phi)$ is the friction coefficient, and D_u is the diffusion coefficient of the activator. We assume[63] that the gel–solvent system satisfies the incompressibility condition, $\nabla \cdot \boldsymbol{v} = 0$; in addition, we set the total velocity, $\boldsymbol{v} \equiv \phi \boldsymbol{v}^{(p)} + (1 - \phi)\boldsymbol{v}^{(s)} = 0$.[48] In other words, it is solely the polymer–solvent inter-diffusion that contributes to the gel dynamics[48,63] and, correspondingly, there is no net momentum exchange between the gel and the external fluid. Hence, by setting $\boldsymbol{v} = 0$,[48,63] we neglect the hydrodynamic interactions within the gels.[64] The hydrodynamic effects in the gels are indeed small; in fact, neutral, non-responsive polymer gels were utilized as a medium for the BZ reaction to specifically suppress the hydrodynamics effects.[34]

Based on the above assumptions, we find the polymer velocity $\boldsymbol{v}^{(p)}$, as:

$$\boldsymbol{v}^{(p)} = \Lambda_0(1 - \phi)(\phi/\phi_0)^{-3/2}\nabla \cdot \hat{\boldsymbol{\sigma}}, \tag{13}$$

where Λ_0 is the mobility coefficient.[48] The stress tensor in eqn (13) is derived from the free energy density of the deformed gel, which consists of the elastic energy associated with the deformations of the polymer network and the polymer–solvent interaction energy. The resulting expression for the stress tensor is:[48]

$$\hat{\boldsymbol{\sigma}} = -P(\phi, v)\hat{\boldsymbol{I}} + c_0 v_0 \frac{\phi}{\phi_0}\hat{\boldsymbol{B}} \tag{14}$$

where $\hat{\boldsymbol{I}}$ is the unit tensor, $\hat{\boldsymbol{B}}$ is a strain tensor, c_0 is the crosslink density of the gel, v_0 is the volume of a monomer unit and ϕ_0 is the polymer volume fraction in the undeformed state. The pressure $P(\phi,v)$ is obtained as:[47]

$$P(\phi,v) = -[\phi + \ln(1 - \phi) + \chi(\phi)\phi^2 - \chi^* v\phi] + c_0 v_0 \phi(2\phi_0)^{-1} \tag{15}$$

The osmotic term (in the square brackets) depends on $\chi(\phi) = \chi_0 + \chi_1\phi$, which is derived from the Flory–Huggins parameter for the polymer–solvent interactions. The parameter $\chi^* > 0$ describes the hydrating effect of the metal-ion catalyst and captures the coupling between the gel dynamics and the BZ reaction. The last term on the right side of eqn (15) describes the pressure from the elasticity of the network.

Numerical integration of the above equations, which describe the dynamics of the chemically reacting gels, can be performed using our recently developed gLSM[48,49] approach. This method combines a finite element approach for the spatial discretization of the elastodynamic equations and a finite difference approximation for the reaction and diffusion terms. The above formalism allows us to simulate an isolated, single gel sample (although this gel sample can be heterogeneous, *i.e.*, contain reactive patches embedded within a neutral gel matrix[54,65]).

To model the solution-mediated communication among multiple pieces of BZ gels in solution, we recently combined this gLSM technique with a finite difference approach that accounts for the diffusive exchange of activator u between the gels and fluid, and captures reaction–diffusion processes occurring in the solution.[66] The details of these model modifications are given in Section 4 below, followed by the results of computer simulations on the communication among the multiple BZ gel samples that are either attached to a substrate, freely slide along a substrate, or suspended in solution. Before presenting the results of these computer simulations, we first review current experimental advance for solution-mediated communication among multiple BZ gels.

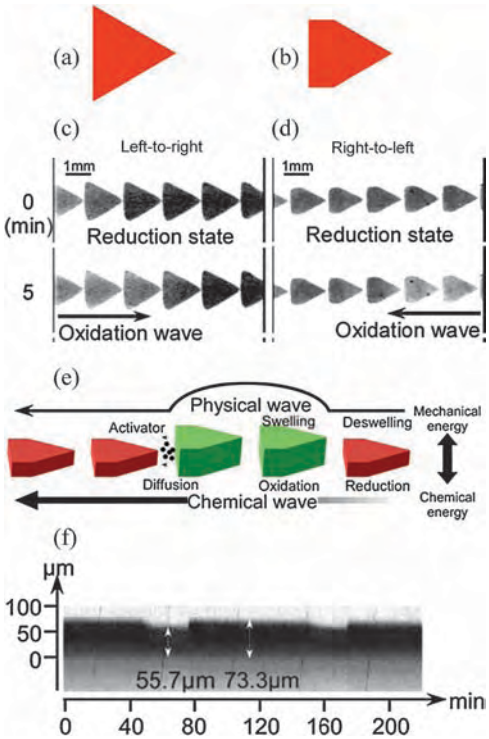

Fig. 1 Propagation of unidirectional chemical waves in the BZ gel arrays consisting of: (a) triangular and (b) pentagonal gel pieces. The wave propagates from the left to the right in the triangular gel array (c), and from the right to the left in the pentagonal gel array (d). (e) Propagating chemical waves are accompanied by periodic changes in the volume of the gels (schematics). (f) The thickness of a pentagonal gel exhibits a roughly 30% variation in volume in the course of the wave propagation. Reprinted with permission from ref. 68. Copyright (2008) of the American Chemical Society.

3. Transduction and communication among multiple stationary BZ gels

The ability of isolated BZ gels to communicate with each other through the surrounding solution has been demonstrated in a number of experimental studies.[67–71] In the ensuing discussion, we first describe the experimental evidence for communication among multiple BZ gels that are bound to a solid surface, focusing on communication between millimeter-sized pieces of different shapes. We also discuss the interactions in a three-dimensional BZ gel that encompasses "projections", which broadly resemble biological cilia. In the following section, we describe computational modeling studies that reveal a novel collective bending in BZ cilia. Finally, we discuss the findings from our modeling studies on the behavior of BZ gels that are not bound to the surface and hence, can undergo net motion in response to the self-generated chemical gradients.

3.1 Passage of chemo-mechanical waves through adjacent samples

We first focus on the inter-gel communication along a row of triangular or pentagonal gels that was demonstrated by Yoshida *et al.*[68] As shown in Fig. 1, this communication led to a concerted response: the propagation of a unidirectional chemical wave within the system. In these experiments, linear arrays of millimeter-sized triangular (Fig. 1a) or pentagonal (Fig. 1b) BZ gels chemically bonded to a glass plate were fabricated using a UV patterning technique.[68] When the gels were immersed in a solution with the BZ reagents, the researchers observed a unidirectional propagating wave of oxidation along the BZ gel array, given that the gels were placed sufficiently close to each other (closer than 220 μm for these experimental conditions[68]). This oxidation wave indicated that Ru catalysts within neighboring pieces became oxidized in a sequential manner, with the oxidation in one piece helping to trigger the oxidation in the neighboring gel. The direction of propagation for this oxidation wave depended on the gels' shape. In the array of triangular gels, the wave propagated from the left to the right (see Fig. 1c), with the wave passing from the corner side of a triangle and to the plane side of the neighboring unit. In the array of pentagonal gels, the waves propagated in the opposite direction, moving from right to the left (see Fig. 1d).

The propagation of the chemical wave along the BZ gel arrays was accompanied by periodic changes in the volume of the gels, as illustrated in Fig. 1e. Namely, the gels underwent a swelling as the catalyst in each adjacent piece became oxidized; the gels then underwent a deswelling as the catalyst was reduced by the periodic redox reaction. Hence, the system exhibited a pronounced chemo-mechanical transduction, with

the chemical energy from the reaction driving the mechanical (volumetric) changes in the gel. Fig. 1f shows that the thickness of a pentagonal gel exhibits a roughly 30% variation in volume in the course of the wave propagation. The gel size did not swell or translate in the horizontal direction because the gel was chemically bonded to the glass plate. The authors noted that the observed variation in height of the attached BZ gel was larger than the size variation in BZ gels undergoing unconstrained, isotropic self-oscillations.[68]

Yoshida *et al.* offered the following explanation of the observed phenomena.[68] Because some of the BZ reaction products inhibit the reaction, the chemical waves tend to originate at the gel boundaries where the concentration of the inhibitors is reduced due to their diffusion to the outer solution.[68] The gel's shape affects the location at which the waves originate because the diffusive exchange is more efficient at a corner than at the plane side, and a sharp corner is more efficient than an obtuse one. The sequential placement of the BZ gel pieces amplifies the wave pattern within each individual gel piece, so that the wave propagates along the array in a direction that depends on the gels' shape. Illustrative simulations, which utilized the 2D Oregonator model of the BZ reaction in solution, were used to support the arguments.[68]

We emphasize that the communication among the discrete, stationary BZ gels described above occurs through the chemical species that are produced by the BZ reaction within the gel pieces and diffuse into the surrounding solution. This form of diffusion-mediated communication depends on the separation between the BZ gels; importantly, the communication did not occur when the separation between the gels exceeded a critical distance, which depends on the concentrations of BZ reactants in the solution. Finally, we note that such chemically initiated communication is not restricted to just BZ gels, and is observed in other heterogeneous BZ systems.[72–77]

The experiments performed by Yoshida *et al.*[68] provided the first evidence that the dynamic behavior of a system of many self-oscillating BZ gels could be engineered by tailoring the shape and spatial arrangement of the constituent pieces. The fabrication technique developed in the latter study opened a new route to creating novel biomimetic chemomechanical devices based on the self-oscillating gels.[9]

3.2 Ciliary motion in BZ gels

A distinctly biomimetic BZ system was fabricated by Tabata *et al.*,[70] who created a surface of self-oscillating cilia-like structures. Through these studies, the researchers demonstrated not only the feasibility of fabricating BZ gels that exhibit complex 3D structures, but also that these artificial cilia could undergo a coordinated motion, mimicking in a general sense the concerted movement of biological cilia. By combining an approach called "moving mask deep X-ray lithography" (M^2DXL) with a micro molding technique, Tabata *et al.* could create the BZ gel "cilia" and surface shown in Fig. 2a.[70] Each "cilium" has a height of 300 μm and a bottom diameter of 100 μm.[70] The cilia exhibited a rhythmic motion as a wave of local swelling propagated along the bottom BZ gel layer, as shown schematically in Fig. 2b. The ciliary motion is evident in Fig. 2c, which shows the trajectory of a cilium tip measured during one

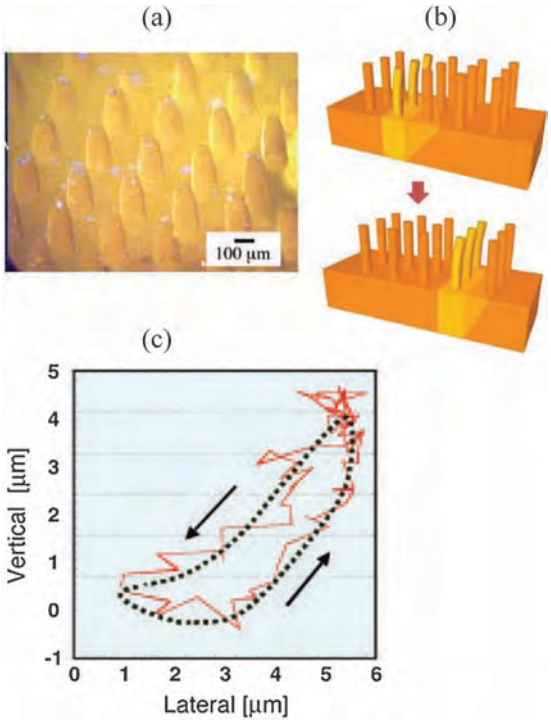

Fig. 2 A ciliary motion actuator[70] fabricated from the self-oscillating BZ gel. (a) A gel plate with micro projection structure array (cilia) on its surface. (b) A ciliary motion as the wave of local swelling propagated along the gel plate (schematics). (c) The measured trajectory of the tip of a cilium. Reprinted from ref. 9. Copyright (2010) with permission from John Wiley and Sons.

actuation cycle.[71] The top of the cilium moved 5 μm in both the lateral and vertical directions, and the trajectory was close to elliptical in shape (Fig. 2c). The movement of these structures arises from traveling chemical waves that traverse the BZ gel substrate and pass up through the cilia; due to the directed motion of these waves along the length of the sample, the columns of cilia move in a sequential manner. In other words, a chemical signal is passed from one column to the next, with the system apparently transmitting a message along the array.

The researchers[70] attributed the observed cilial motion primarily to the propagation of the swelling–deswelling deformation through the base BZ gel layer. In other words, the ciliated surface in Fig. 2 is a single BZ gel sample that entails a complex geometry, where portions of this sample (cilia) communicate through the surrounding solvent and the flat, lower layer. This scenario is distinctly different from the system described in Section 4, where we model BZ gel cilia attached to a rigid, non-reactive substrate and these cilia communicate solely through the surrounding solution. The actuation of BZ cilia could prove valuable for microfluidic applications. In particular, the BZ cilia array could be used for transporting microparticles on the surface within a microfluidic device.

3.3 Mechanical stimulation of the BZ reaction in non-responsive media

In the above discussions, we emphasized that the BZ gels transduce the chemical energy from the BZ reaction into the

mechanical energy of shape or volume change, allowing the system to produce useful work; for example, as noted above, the oscillating surfaces can serve as a conveyor belt that transports objects along the length of the sample.[78,79] Given the robust exchange of chemical and mechanical energy in these systems, one might anticipate that the BZ gels should also be capable of mechanochemical transduction, converting mechanical energy into chemical energy. In other words, an external mechanical action could affect the internal chemical activity within the gels. The latter form of energy transduction was observed in non-responsive gels that served as media for the BZ reaction (*i.e.*, the gels did not respond to the chemical oscillations by swelling and deswelling). In particular, an instance of mechanically altered chemical response in a BZ elastic medium was first observed in a polyacrylamide–silica composite gel where the BZ catalyst (ferroin) was immobilized in the silica nanoparticles.[80] After immersion into a solution of the BZ reagents and initiation of the spiral waves, the gel was stretched uniaxially, at specific fixed frequencies of mechanical loading. The spatial position of the BZ spiral waves shifted when this loading frequency was comparable to that of the spiral angular frequency.[80] While this mechanical stimulus altered the BZ wave, there was no direct transduction of mechanical to chemical energy since the mechanical stretching failed to initiate a chemical wave.

Another example of the mechanical stimulation of a BZ system involves ferroin that is immobilized in a commercial, cation-exchange membrane known as Nafion™.[81] The catalyst-containing membrane was immersed in a BZ solution; with the specified stoichiometry, the BZ reaction was in the excitable regime in the membrane. Thus, the membrane exhibited no oscillatory chemical activity under quiescent conditions. However, as illustrated in Fig. 3, when Suzuki *et al.* pressed the membrane with the tip of a glass stick, a chemical wave was induced in the pressed area. It was possible to trigger additional chemical waves by repeatedly applying mechanical force to the membrane. The material, however, required 30 min of recovery time to restore the capacity for mechanical responsiveness.[81]

These studies hinted at the possibility that a mechanical cue could trigger chemical pulsations in BZ gels, a behavior which would enable a range of novel pressure sensors. In fact, recent computational studies also predicted that chemoresponsive BZ gels could be driven to oscillate by an applied force.[82,83] Recently, these predictions have been verified experimentally.[69] Furthermore, these experiments showed mechanically induced signaling among multiple gels;[69] these findings are discussed in more detail below.

3.4 Mechanically initiated oscillations and communication in multiple BZ gels

As demonstrated by Suzuki *et al.*,[81] BZ membranes containing immobilized catalyst are capable of transducing mechanical energy into the chemical energy of the BZ reaction for a single target wave. It is, however, also possible to achieve conditions wherein mechanical pressure results in robust BZ oscillations within a previously quiescent gel. To prepare a mechanically triggerable BZ gel, the chemical conditions of the experiment can be tuned by priming the gel in a BZ solution overnight. Chen *et al.* have demonstrated this behavior for a mm-scale NIPAAm-based BZ gel disc that was exposed to chemical reagents (malonic acid, sodium bromate, and nitric acid), and was allowed to self-oscillate for 20 h.[69] After undergoing the BZ reaction for many hours, chemical reactants were consumed while inhibitor species were produced, resulting in exhaustion of oscillations within the gel. Note that the gel remained submerged in a solution containing chemical reactants, but that the chemical supply was partially depleted by the reaction occurring over 10s of hours. The state of the gel was confirmed by monitoring the gel hue, a specific mathematical definition of color that is an indicator of the chemical oxidation state of the $Ru(bpy)_3$ catalyst. Uniaxial compressive stress was applied to the non-oscillatory gel by placing a series of glass cover slips of known mass on top of the gel disc, triggering BZ oscillations. Oscillations ceased when the glass cover slips that exerted the compressive load was removed.[69] Although one could reasonably question whether this method of applying mechanical load to the sample instead triggered oscillations by changing diffusive conditions (*i.e.*, the glass slide serving only as a diffusion barrier), this possibility was ruled out by showing that the BZ oscillations were triggered only by stacking enough glass slides to achieve a specific applied load; a single coverslip was sufficient to limit diffusion of species through the topmost gel surface, but insufficient to trigger chemical oscillations.

To demonstrate the pressure sensing capability of BZ gels, four discrete gel discs (of 0.7 mm diameter) were prepared and placed on the bottom of a Petri dish. The discs were placed more than 1 mm apart from each other and submerged in a BZ solution overnight (Fig. 4A). After 20 h, the state of each gel was confirmed by monitoring its hue, and each disc was no longer oscillating. The hue of the gel discs was quantified to detect the time and location of mechanical loading within the system. For instance, compression was applied to only disc 1 after

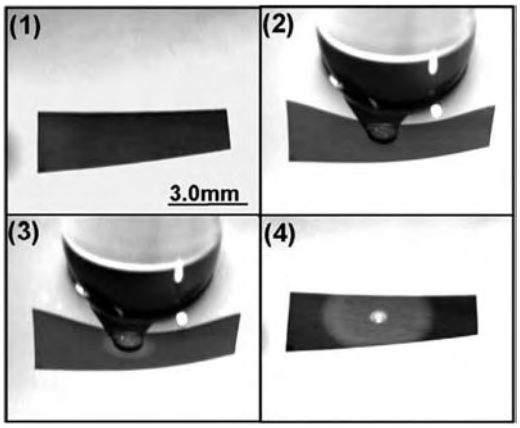

Fig. 3 Induction of chemical waves by mechanical stimulation in elastic BZ media based on *Nafion* membrane loaded with the catalyst ferroin. The successive photographs of the process made at an interval of 60 s (tip radius 0.44 mm, tip force 3.26 N). Reprinted from ref. 81. Copyright (2001), with permission from Elsevier.

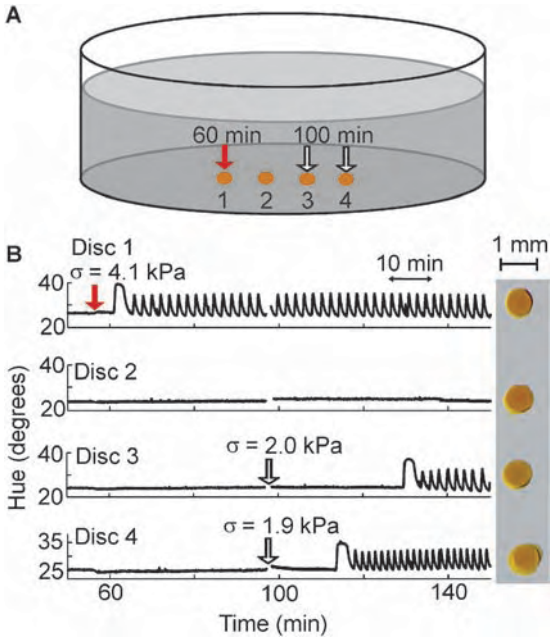

Fig. 4 Mechanically triggered oscillations in stationary BZ gel discs. (a) Schematic of experiment showing that four BZ gel discs were submerged in a solution with BZ reagents while disc 1 was mechanically triggered at t = 60 min, followed by mechanical triggering of discs 3 and 4 at t = 100 min. (b) Oscillations in discs 1, 3 and 4, and non-oscillatory state in disc 2. Mechanically triggered oscillations in discs 1, 3 and 4 were not communicated to disc 2. Reprinted from ref. 69. Copyright (2012), with permission from Wiley.

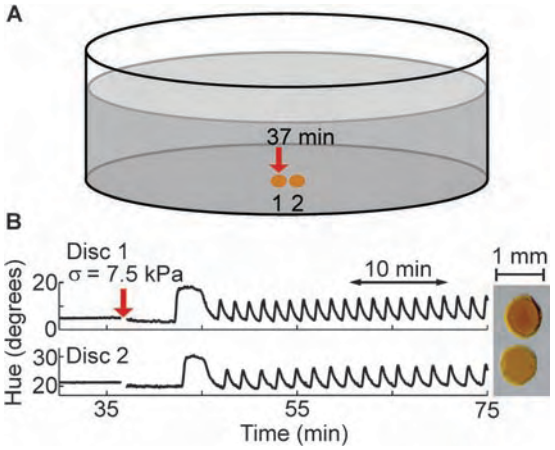

Fig. 5 Mechanically triggered communication in stationary BZ gel discs. (a) Schematic of experiment showing that two BZ gel discs were submerged in a solution with BZ reagents while disc 1 was mechanically triggered at t = 37 min. (b) Oscillations in discs 1 and 2 demonstrating that the mechanically triggered oscillations in disc 1 induce oscillations in disc 2. Such communication between BZ gels occurs when the gap distance between discs is 0.23 mm. Reprinted from ref. 69. Copyright (2012), with permission from Wiley.

approximately 60 min of confirming the lack of BZ oscillations (*i.e.*, 21 h after the gels were immersed in the BZ solution), and colorful oscillations were triggered only in disc 1. Similarly, discs 3 and 4 exhibited BZ oscillations after approximately 100 min, correlating with the approximate time when compression was applied only to these gels (Fig. 4B). Gel 2 was uncompressed and remained in the non-oscillatory state (Fig. 4B). Thus, the oscillatory color changes of the BZ gels were harnessed in a position-sensitive pressure sensor comprising discrete BZ gel discs.[69]

Not only can BZ gels detect mechanical stimuli, but these gels can also transmit oscillatory signals away from the triggered site. To demonstrate the signaling capability of BZ gels, Chen *et al.* placed two gel discs close to each other (0.23 mm gap distance) and submerged these in BZ solution overnight (Fig. 5). Again, the exhaustion of BZ oscillations within each gel was confirmed by monitoring gel hue. When compression was applied only to disc 1, the color response in disc 1 was followed by color change in disc 2. Both discs oscillated due to signal transmission across the gap *via* chemical diffusion of activator species produced by the BZ reaction. The period of oscillation for discs 1 and 2 was 1.5 min and 1.8 min, respectively, and the amplitude of oscillations was 8.9° and 6.7°, respectively.[69] Thus, these details of the BZ reaction did not differ appreciably between the gel in which the BZ oscillations were mechanically triggered and the gel in which the BZ oscillations were communicated chemically. Note that, as in the case of chemically initiated BZ reactions among gels noted by Yoshida *et al.* in Fig. 1, the signal transmission capacity between the discs in Fig. 5 depended on the distance separating the gel edges. For the conditions discussed above, Chen *et al.* found that a separation of 0.3 mm was too large for chemical signaling between the gels to occur.

The signaling capacity of BZ gels is not limited to propagation from the nearest neighboring gel, but rather depends ostensibly on whether this separation exceeds the diffusion distance of BZ species. Fig. 6 shows that when Chen and Van Vliet placed additional gels next to the mechanically triggered gel, wave propagation occurred in all of the neighboring discs, provided that the discs were within the critical separation distance. The magnitude of this critical distance depends on several details, including the catalyst concentration in the gel and the BZ solution concentrations of activator and inhibitor species; for the conditions in Fig. 6, the four gel discs (of 0.7–0.8 mm diameter) were arranged in a 2 × 2 matrix with nearest-neighbor edge spacing being less than 0.2 mm. Unlike Fig. 4 and 5, the mechanically triggerable state was not achieved *via* overnight depletion of reactants upon exhaustion of the BZ oscillatory reaction. Instead, a small amount of inhibitor species (3 mM) was added to the external solution and mixed with BZ reactants. Such chemical conditions resulted in a non-oscillatory BZ gel system. As described previously, macroscopic compression was applied to only one BZ gel to observe wave propagation to neighboring gels. The gap distances between neighboring discs were no more than 0.16 mm, and when the bottom right disc (labeled a in Fig. 6) was mechanically triggered, all four discs exhibited BZ oscillations in a temporally delayed fashion that depended on the distance from this compressed gel. Color change was sequential, occurring first in the triggered gel (labeled a), and then followed by propagation to the bottom left and top right gels (labeled b and c, the nearest neighbors), and then finally ending with propagation to the top left gel

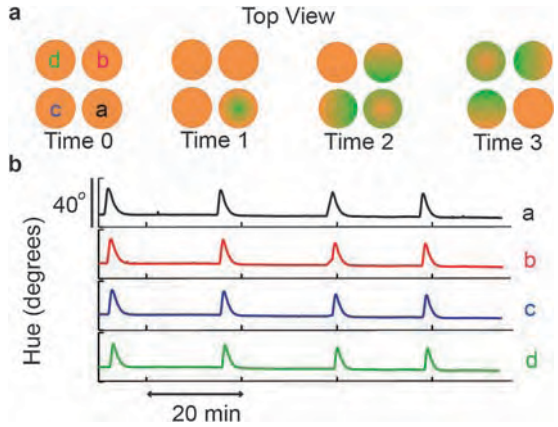

Fig. 6 Mechanically triggered oscillations and signal propagation in BZ gels. (a) Schematic of experiment indicating sequential order of wave propagation (shown in green) in gels a–d. Indicated time points 0–3 are unitless and do not reflect the actual period of oscillation or wave velocity. (b) Hue of gels a–d, demonstrating actual wave propagation in gels. Due to the long period of oscillation, it is difficult to see that gel a did indeed oscillate first, followed seconds later by gels b and c. Gel d oscillated seconds after gels b and c.

(d, the next-nearest neighbor). This sequential propagation shows that the signaling did not occur directly across the 0.52 mm distance between gels a and d, and consequently, the critical gap distance for these conditions was smaller than 0.52 mm.

Together, such recent experiments demonstrate that mechanical load (at least uniaxial mechanical compression) can trigger chemical oscillations in a BZ gel, and that these oscillations can be transmitted chemically to adjacent gels.[69] This mechanically triggered BZ oscillatory behavior is reminiscent of mechanical resuscitation of a heart, though this analogy has obvious limitations. Further note that this sensing and signaling capacity in stationary gels evokes biological phenomena such as the mechanically induced Ca^{2+} signaling among adjacent osteocytes *in vitro*[84] or among slime molds, though again the details of the underlying chemical reactions differ appreciably. Whether such engineered behavior of BZ gels is leveraged as a model of biological systems or is instead exploited as a new material for mechanical sensing and signal propagation, the capacity to both transduce and transmit mechanical cues *via* chemical signals is an exciting step forward in synthetic, stimuli-responsive materials.

4. Communication among BZ cilia

The above studies highlight recent experimental evidence for chemical signaling in systems of BZ gels. In the following sections, we describe recent theoretical and computational studies that point to both communication and auto-chemotactic behavior in these systems. The first example involves artificial cilia that are formed from BZ gels; just as in the case of biological cilia, these hair-like structures are anchored to a substrate. Hence, cilia cannot exhibit a net lateral displacement. Nonetheless, we find that the movements of BZ cilia depend on the self-generated, local variations in u, the activator for the reaction (see Section 2). In particular, the direction of wave propagation within a single cilium, as well as groups of cilia, is controlled by the local distribution of u.[66] Additionally, the BZ cilia undergo an auto-chemotactic bending; namely, they bend toward the highest concentrations of u in the surrounding solution.[66] There is another distinctive feature of the BZ cilia: the gels are photosensitive.[62] By selectively illuminating specific cilia in an array, we can control the pattern of wave propagation within the system. In effect, the motion of the tops of the cilia resembles the movement of piano keys, with the light serving to control the "tune."[66]

Below, we first describe the modifications we made to the gLSM model to capture the complex behavior of the BZ cilia.[66] This model is also used to describe the behavior of the unattached, freely moving auto-chemotactic gels that are described in Section 5.

4.1 Methodology and model parameters

To model the BZ cilia in solution, Dayal *et al.* recently combined the gLSM technique with a finite difference approach that accounts for the diffusive exchange of u between the gels and fluid, and captures reaction–diffusion processes occurring in the solution.[66] Hence, we could capture the interplay between the pulsations of the cilia and the dispersion of u, where the motion of the cilia affects the distribution of u, which in turn affects the movement of the cilia.

The evolution of the activator concentration, u, outside the gels and within the external fluid is given by

$$\frac{\partial u}{\partial t} = \nabla^2 u - u^2 \qquad (16)$$

The last term on the right hand side represents the decay of activator due to the dis-proportionation reaction.[72,85] We focus only on reaction–diffusion processes in the outer fluid and neglect the effects of hydrodynamics. In the simulations presented below, the dimensionless velocity of the gel's expansion/contraction is approximately 0.1, which corresponds to approximately $\mathbf{v} = 8\ \mu m\ s^{-1}$ using the scaling provided below.[66] If hydrodynamic effects were taken into account, one would expect the characteristic velocities created in the fluid by the cilia motion to be of the same order of magnitude as this $\mathbf{v}$, which in turn would correspond to a low Reynolds numbers of[66] $Re \sim 10^{-2}$ (assuming the viscosity of the solution equals that of water and taking the length of the cilium, 1.3 mm (see below), to be the characteristic length scale). The hydrodynamic forces acting from the fluid on the gel surface would be negligibly small due to the low ratio of viscous to elastic forces; this ratio, the relevant capillary number[86] can be estimated as[66] $Ca \sim 6 \times 10^{-11}$, where the bulk modulus of the NIPAAm gel is taken to be 10^5 Pa,[87] and again the length of a cilium is taken as the characteristic length scale. Hence, due to the slow dynamics of the gels and low viscous forces, we can neglect hydrodynamic effects.[66]

Eqn (8)–(10) are the governing equations for the polymer–solvent system and are solved solely inside the gel, on a Lagrangian grid. The deformable hexahedral elements of this grid are defined by gel nodes. Eqn (16) is solved solely in the fluid, on a fixed, regular, Eulerian grid. At every time step, the flux of activator from the fluid to the gel is interpolated from the Eulerian grid, while the flux of activator from the gel to the

fluid is interpolated from the Lagrangian grid. For the surfaces of the Lagrangian grid that are attached to the wall, we impose no-flux boundary conditions for the activator. These boundary conditions allow for the exchange of activator between the fluid and gel only across the mobile gel–fluid interfaces. We use no-flux, Dirichlet or periodic boundary conditions for the external boundary on the fluid grid. In the examples below, unless specified otherwise, we impose no-flux boundary conditions for the activator, u, at the bottom wall of the simulation box and set $u = 0$ at the rest of the walls.

Where possible, the systems parameters are taken from known experimental data. In particular, for the BZ reaction parameters, we set[48,53] $\varepsilon = 0.12$, $f = 0.9$ and $q = 9.52 \times 10^{-5}$ and for the parameters characterizing the properties of the gel, we set $\phi_0 = 0.139$, and $c_0\nu_0 = 1.3 \times 10^{-3}$ (based on experimental data provided in ref. 18). For the interaction parameters in eqn (16), we used $\chi_0 = 0.338$ and $\chi_1 = 0.518$, which corresponds to the NIPAAm gel–solvent interaction parameters at 20 °C for a gel with the above values of ϕ_0 and c_0.[87] We also set $\chi^* = 0.105$; χ^* is an adjustable parameter of the model and is chosen to have the same value as in ref. 48, 51, 52 and 55. For the initial conditions within the gels, we chose the concentrations of the oxidized catalyst and activator to be randomly distributed around their stationary solutions for the given reaction parameters,[49] $\nu_{st} = 0.18$ and $u_{st} = 0.19$, and we set the initial degree of swelling λ to its stationary value $\lambda_{st} = 1.75$. To determine the characteristic length and time scales of the system, we assume that the diffusion coefficient of the activator,[48] $D_u = 2 \times 10^{-9}$ m^2 s^{-1}, remains the same in the gel and surrounding fluid.[88] Using the above values, our dimensionless units of time and length correspond to the respective physical values of $T_0 = 0.31$ s and $L_0 = \sqrt{D_u T_0} = 25$ μm.

4.2 Results and discussion

Recall that the activator u is generated within the gel during the course of the BZ reaction and diffuses from the gel to surrounding solution. These processes lead to local variations in u. As we show below, whether it is the pulsations of a single cilium or the collective bending of multiple cilia, these filaments not only sense, but also move in response to the local gradients in u.[66] In effect, these artificial cilia mimic the ability of biological species to direct their motion along chemical concentration gradients.

4.2.1 Response of a single cilium to variations in *u*. We begin by considering a single BZ cilium immersed in solution, as shown in Fig. 7. The size of the cilium is $(5 \times 5 \times 29)\lambda_{st}$, where $\lambda_{st} = 1.75$ denotes the gel's initial degree of swelling. The activator concentration is specified at the top boundary of the box ($u = u_{top}$) and is maintained at $u = 0$ at all the other fluid boundaries. The images in Fig. 7 represent wave propagation at late times in three independent simulations. When the activator concentration is zero at the top fluid boundary ($u_{top} = 0$, left image), at late times, the traveling wave propagates from the fixed to the free end. This phenomenon is consistent with experiments on a single, long rectangular BZ gel attached to a wall,[8] and with our earlier computer simulations on single, end-tethered BZ gels.[48,49,53,89] When the activator concentration is increased to moderate values ($u_{top} = 0.02$, central image), at late times, the traveling waves emerge simultaneously from both the ends of the sample. In each cycle, the waves travel towards the center of the gel, where they meet and annihilate each other. With a further increase in the activator concentration at the top boundary ($u_{top} = 0.1$, right image), the traveling waves now emerge from the free tip and travel towards the fixed end.

The phenomena observed in Fig. 7 can be explained as follows.[66] The oscillation frequency, ω, of a small, isolated BZ gel increases with the concentration of u in the outer solution.[66] In other words, the chemo-mechanical oscillations in the gel occur at a higher frequency when the concentration of the activator in the surrounding fluid has a higher value. Furthermore, in a system containing multiple oscillators, the region with the highest frequency determines the ultimate direction of wave propagation.[90,91] In our BZ cilium, each element acts as an oscillator, and the intrinsic frequency of this oscillator depends on the boundary values of u in the outer fluid and neighboring elements. (The intrinsic frequency[66] of a small region of the gel refers to the frequency of the oscillations that an isolated gel of the same size would exhibit if it were placed in a fluid with the same value of u.) For $u_{top} = 0.0$, the fixed end of the gel has the highest intrinsic frequency and hence, the traveling waves propagate bottom-up. In the case of $u_{top} = 0.1$, the free end of the gel has the highest intrinsic frequency, and consequently, the waves travel top-down. For the moderate the case where $u_{top} = 0.02$, the waves emanate from both ends since the concentration of u is comparable near the fixed and free ends of the cilia. Fig. 7 clearly demonstrates that the local

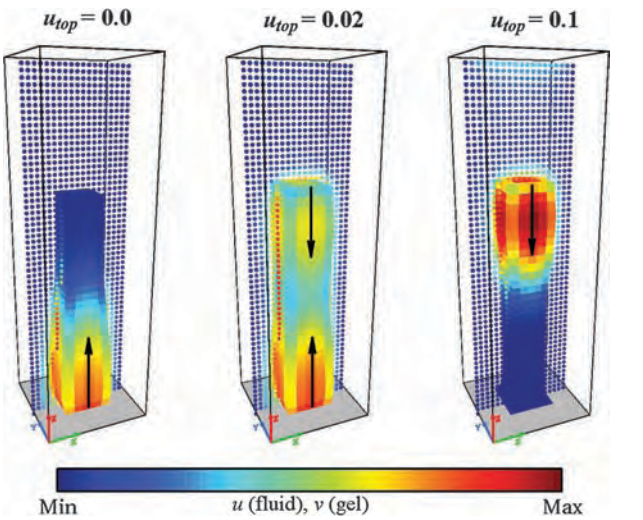

Fig. 7 Late time snapshots of BZ cilium (6 × 6 × 30 nodes) immersed in solution; the activator concentration is specified at the top boundary of the box ($u = u_{top}$) and is maintained at $u = 0$ at all the other fluid boundaries. Here and below, the oxidized catalyst concentration (v) on the gel's surface and the activator concentration (u) across the central plane of the fluid box are mapped using the color bar; the minimum values (in blue) are always set to zero, while we vary the maximum values (in red) as provided in each case. Here, we set $u_{max} = v_{max} = 0.3$ for $u_{top} = 0.0$ and 0.02 and $v_{max} = 0.18$ for $u_{top} = 0.10$. Here and below, the black arrows represent the direction of the traveling wave.

activator concentration in the fluid determines the directionality of wave propagation in the cilium.

4.2.2 Probing the behavior of two interacting cilia. Since our aim is to determine the factors that control the inter-cilial communication, we now focus on two BZ cilia immersed in fluid (Fig. 8) and examine how the separation between these gels, d, affects the system's behavior. The size of each cilium is $(5 \times 5 \times 29)\lambda_{st}$, where λ_{st} denotes the gel's initial degree of swelling. The diffusive exchange of u between the gel and fluid occurs through all the gel's surfaces in contact with the solution. The parameters b (the spacing between the outer cilia surfaces and fluid boundaries), d and the size of the gel define the length of the simulation box in the x-direction; the length of the box in the y and z directions is fixed at 20 and 63 dimensionless units, respectively. The concentration of u at $x = 0$ and $x = L_x$ is set to zero. Periodic boundary conditions are imposed in the y direction and no-flux boundary conditions are specified in the z direction. Based on the scaling in Section 4.1, the initial size of the non-deformed gels corresponds to approximately 0.2 mm $\times$ 0.2 mm $\times$ 1.3 mm and the distance between the two cilia ranges from 0.09 mm to 0.51 mm (*i.e.*, from 3.5 to 20.5 dimensionless units).

We focus on the two examples shown in Fig. 8, where we fix $b = 5.5$. The color of the dots across the central plane of the simulation box indicates the activator concentration (see color bar in Fig. 7). At early times for both these cases, the chemo-mechanical waves generated by the BZ reaction within the gel travel bottom-up and the wave propagation in the neighboring cilia is synchronized. At late times, however, the behavior in these two examples becomes distinctly different. If the two cilia are placed relatively close together ($d = 3.5$), the waves travel from top to bottom at late times (Fig. 8a). For the two cilia that are placed relatively far apart ($d = 20.5$), the traveling waves at late times are generated at the center of each cilium. Additionally, these waves oscillate out of phase with respect to each other (see Fig. 8b).

Fig. 8c and d show the distribution of u around the cilia, revealing that this distribution is highly non-uniform and depends markedly on d. (The distribution is calculated at a moment in time when the catalyst is predominantly in the reduced state.) When the cilia are located relatively close to each other (Fig. 8a), the highest concentration of u in the fluid is observed above the cilia (Fig. 8c). The relatively low u values between the cilia at small d arise because the fraction of activator, which was produced during the oxidation phase and spread out from the cilia, diffuses back into the gels from the narrow inter-cilial spacing when the catalyst is in the reduced state. For cilia that lay further apart, however, the highest concentration of u is closer to the center of the simulation box (Fig. 8d). With the relatively large space between the cilia, the fraction of u that diffuses back to the gels during the reduction phase constitutes only a small fraction of the total amount of u that is located between the cilia.

Fig. 8c and d also help explain the directionality of wave propagation in the two exemplar cases. For the case of the closely spaced cilia, the higher concentration of u near the tops

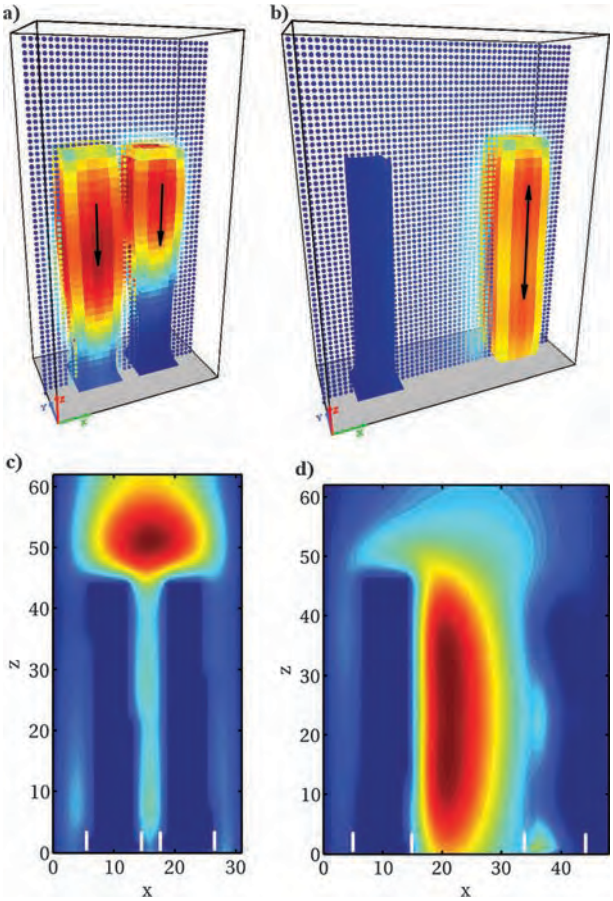

Fig. 8 Effect of the separation between the two cilia, d, on their dynamics. The images in (a) and (b) correspond to late time snapshots for $d = 3.5$ and $d = 20.5$, respectively; (c) and (d) show the distribution of u across the central plane of the fluid box for $d = 3.5$ and $d = 20.5$, respectively. For these images, the catalyst in the cilia is predominantly in the reduced state. The white lines at the bottom of panels (c) and (d) show the position of the bottom cilial surfaces. Here, we set $v_{max} = 0.12$ and $u_{max} = 0.33$ in (a) and (b), $u_{max} = 0.02$ in (c) and $u_{max} = 0.08$ in (d). We fixed the distances to the box boundaries at $b = 5.5$.

of the gels results in higher intrinsic oscillation frequencies close to the free ends and causes the observed top-to-bottom wave propagation, similar to the right most case of a single cilium in Fig. 9. In the case where the cilia lie further apart ($d = 20.5$), the highest concentration of u and consequently, the highest intrinsic oscillation frequency corresponds to the center (in the z-direction) of each cilium. The latter observation helps rationalize the observed late-time wave propagation seen in Fig. 8b, where the waves initiate from the center of the cilia.

The above examples demonstrate that the u-mediated communication between the two cilia affects the direction of wave propagation within each cilium.[66] The distribution of u also effects the relative bending of these filaments; this can be seen more clearly in the cases below.

4.2.3 Investigating the communication among multiple BZ cilia. We expanded our system to encompass five cilia that are arranged along the x-direction with $d = 3.5$ and $b = 5.5$; we again set $u = 0$ at the boundaries. Fig. 9a shows the distribution of u at late times within the system. (This distribution is calculated at

a moment in time when the catalyst within the cilia is predominantly in the reduced state.) Due to the symmetric arrangement of the cilia and the boundary conditions in the x-direction, the average concentration of u is highest in the central portion of the box (see Fig. 9a). The latter distribution of the activator gives rise to a number of distinctive effects. First, as seen in Fig. 9b, the traveling waves propagate from top-to-bottom at late times (since the activator concentration is highest at the top of cilia array). Second, Fig. 9b reveals that the central cilium leads the oscillations within the system (due to the highest level of u being located at the top of this filament). A third effect that indicates a distinctive form of chemotaxis in the system can be seen in Fig. 9b and c: the anchored filaments collectively bend toward the highest concentration of u in the system. The cilia numbered 1, 2 and 4, 5 (numbering from left to right) are effectively "bunched" together as they tilt towards the high concentration of u in the central region (see Fig. 9c).

The bending of these cilia can be attributed to the non-uniform concentration of u in the lateral direction (see Fig. 9a). The gradients across the sample indicate that there is a component of wave propagation in the x-direction. (Note that the wave propagates predominately along the length of the cilia due to the high aspect ratio of these filaments.) In particular, the concentration of u is higher for the inner than the outer surface of the cilia due to $u = 0$ constraint at the boundaries of the simulation box (and consequently, these differences are most pronounced for cilia 1 and 5). Hence, the inner surface has a higher intrinsic frequency and the direction of the lateral component of the traveling wave is from the inner to the outer

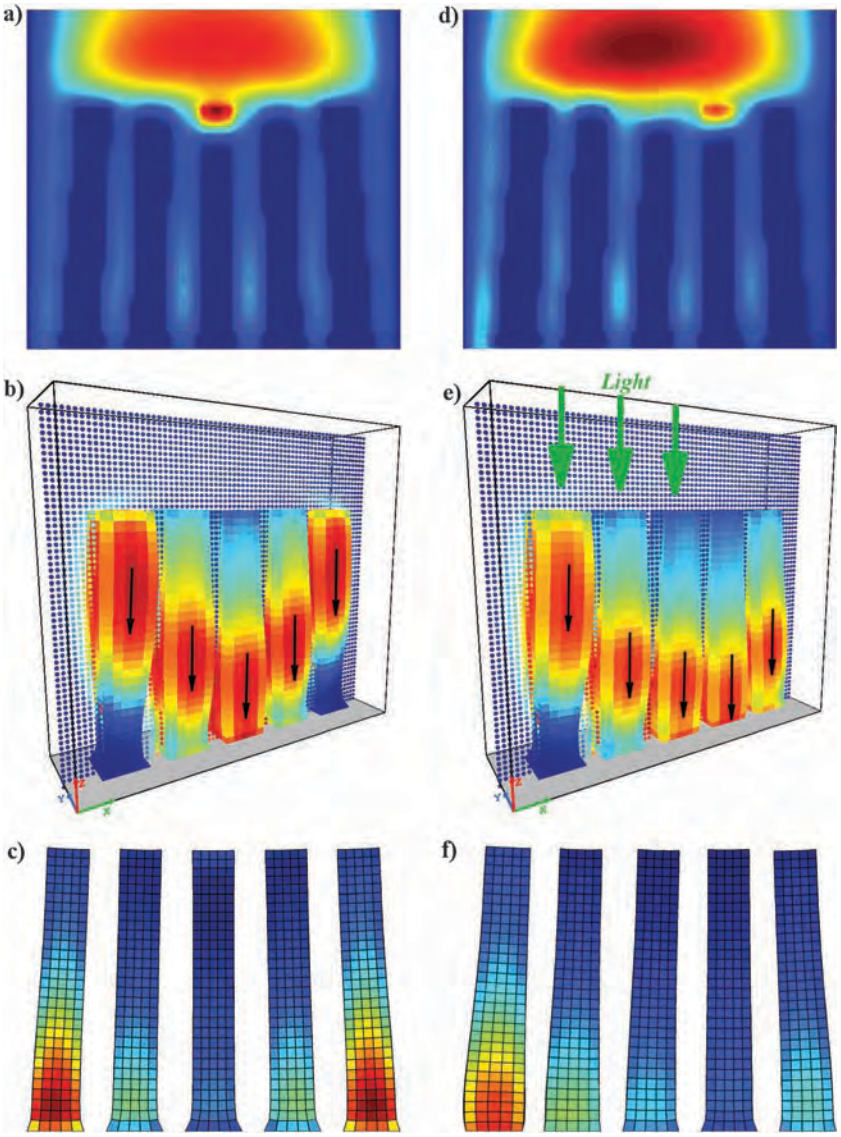

Fig. 9 Dynamics of the five cilia system. The size of the simulation box is 69 × 20 × 63 (in x, y and z directions) with $d = 3.5$ and $b = 5.5$. (a–c) show the late time snapshots in the absence of light ($\Phi = 0$). (d–f) show the late time snapshots when cilia 1, 2 and 3 (numbered from left to right) are illuminated by light ($\Phi = 15 \times 10^{-3}$). Here, we set $u_{max} = 0.038$ in (a), $u_{max} = 0.32$, $v_{max} = 0.20$ in (b), $u_{max} = 0.033$ in (d), $u_{max} = 0.30$, $v_{max} = 0.28$ in (e).

surface of each cilium. The traveling wave effectively "pumps" some amount of solvent from the inner space between the cilia to the outer regions. Due to the inter-diffusion of the polymer and solvent,[48,63] the pumping of fluid in a given direction results in the net motion of the BZ gels in the opposite direction. We have observed this behavior in our previous studies on single BZ gel samples that are free to move.[51,92] Here, however, the bottoms of the cilia are anchored to the substrate. Thus, the induced motion of the solvent (through the cilia) from the area between the cilia to the outer bath drives the cilia to bend in the opposite direction: namely, the cilial tips bend inwards and thus, towards each other.

Fig. 9c depicts a novel form of chemomechanical transduction in this synthetic system, where dynamically evolving chemical gradients in the solution induce a deflection of the cilia and an effective attraction between these anchored gels. As noted above, these cilia display a distinct form of chemotaxis: the self-generated gradient in the activator for the chemical reaction ultimately draws the cilia towards the highest concentration of u.

The "bunching" of the five cilia towards the center of the box is significantly more pronounced than the inward bending of the two cilia (see Fig. 8b). The distinct clustering of the five cilia in Fig. 9b and c can be attributed to the maximum in u being located over the top of the middle cilium (Fig. 9a) rather than spread more uniformly over the tops of two cilia (much as in Fig. 8d). The average values of u in the fluid are also significantly higher in Fig. 9a than for the examples involving two cilia.[66] These factors contribute to relatively large lateral gradients in u, which drives the four outer cilia to cluster towards the central cilium.

The fourth distinctive feature of these 3D systems is that the positions of the top surfaces of all the cilia (their heights, curvature, and the inter-cilia distance) change according to the observed synchronized oscillations.[66] These dynamic changes can be visualized most dramatically by focusing on the vertical displacements of the tops of the cilia and watching as the surfaces move up and down in a complex dynamical pattern, as seen in the example described below.

4.2.4 Communication in the presence of light. The BZ gels are photosensitive; illuminating a sample with light of a specific wavelength gives rise to an additional flux of bromide ions, which inhibits the oscillatory behavior.[62] By increasing the intensity of this light beyond a critical value, the oscillations can be completely suppressed (in the absence of the influx of u to the gels from the surrounding fluid).[62] We now exploit these photo-responsive properties to control the interactions in our array of five cilia, including regulating the rhythmic height variations in the oscillating array.

For the case shown in Fig. 9d–f, the geometric configuration and boundary conditions are the same as in Fig. 9a–c, except that cilia 1, 2 and 3 (numbered from left to right) are illuminated by light. The effect of light is captured in our simulations by setting $\Phi = 1.5 \times 10^{-3}$ (see eqn (11)), which represents the additional flux of bromide ions.[57] This Φ value is greater than the critical value required to curb the production of u and suppress the oscillatory behavior[51] and hence, under these conditions, an isolated cilium would not exhibit chemomechanical oscillations. The oscillations in the five cilia array in Fig. 9c and d would also be suppressed if the entire array were illuminated with uniform light corresponding to this value of Φ. In Fig. 9e, however, the non-illuminated cilia (numbered 4 and 5) continue to produce the activator u, which diffuses through the fluid to cilia 1, 2 and 3. As the concentration waves travel from right to left (in the negative x direction), the local activator concentration increases sharply and thereby switches "on" each cilium.

Once the concentration of u builds up in the system, the waves travel synchronously from the top to bottom of the cilia length (as marked by arrows in Fig. 9e). Due to the light source, the leading wave front shifts towards the non-illuminated side. Here, all the cilia are effectively coming closer together, similar to the case in Fig. 9c; however, the middle cilium is also somewhat tilted (see Fig. 9f) because the distribution of u surrounding this central cilium is asymmetric, as seen in Fig. 9d.

To gain further insight into the collective dynamics of the illuminated cilia (Fig. 9d–f), it is useful to refer to our prior studies[66] on the behavior of a small, isolated BZ gel cube in the presence and absence of light as we systematically increased u in the outer solution. We found that the oscillation frequencies, ω, for the non-illuminated and illuminated samples were quite similar; hence, the overall change in the direction of wave propagation in both samples is driven by the increase in u near the free surfaces at late times.[66] On the other hand, ω in the presence of light remains lower than that in the absence of light for a wide range of u.[66] The latter observation explains both the shift in the position of the leading front towards the cilia in the dark (see Fig. 9e), as well as the asymmetric "bunching" of the cilia towards the non-illuminated region (Fig. 9f).

The dynamic variations in the behavior of the cilia at early times can be seen from a top-down view. In particular, the height of each cilium increases, reaches the maximum value when the catalyst is in the oxidized state and then decreases when the catalyst is in the reduced state. We call this variation in height the "piano effect"[66] since the cilia appear to move up and down like the keys of a piano. To illustrate this piano effect, in Fig. 10 we plot the temporal behavior of the top cilial surfaces corresponding to the case in Fig. 9e. This image in Fig. 10 shows the pronounced transient pattern that occurs while the activator concentration in the fluid remains relatively low, *i.e.*, until about $t \sim 10^3$, which corresponds to more than a dozen oscillation cycles. Each cilium reaches its corresponding maximum height in a sequential manner. The fact that the light source causes the leading wave front to shift towards the non-illuminated side is also reflected in the variations of heights of the cilia.

In summary, through these studies, we demonstrated that the BZ cilia exhibit a remarkable chemo-sensing capability and ability to autonomously translate this chemo-sensitivity into a distinct mechanical response. These attributes could be usefully exploited in a range of microfluidic applications, where, for example, an external light source could be utilized to tailor the movement of a soft "conveyor belt"[78,79,93] and thus, regulate the transport of microscopic objects within the devices.

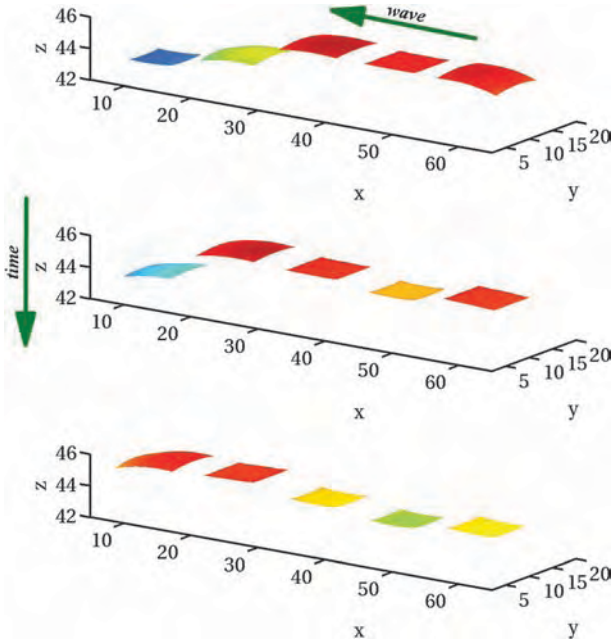

Fig. 10 The ''piano'' effect. Variation of the positions of the top cilial surfaces at early times when cilia 1, 2 and 3 (numbered from left to right) are illuminated by light ($\Phi = 15 \times 10^{-3}$). Each cilium reaches its corresponding maximum height in a sequential manner and appears to move like the keys of a piano.

5. Communication among multiple mobile BZ gels

In contrast to the examples above, we now consider systems of closely spaced BZ gels that can slide freely on the underlying substrate. In such a system, the substrate could be functionalized chemically to not only prevent the gels from sticking to the surface, but also allow the gels to move along the surface with relatively little or no friction. In these studies, we use the computational model outlined in Section 4.1; the model, however, was recently modified[3] to prevent the freely moving pieces from colliding and penetrating into each other. In particular, we introduce an inter-gel interaction,[3] which is based on the repulsive part of the Lennard-Jones potential, between nodes on different gels that lie within a critical distance of each other. By introducing these excluded volume interactions between mesoscopic pieces, we can readily capture the late-time behavior of the system, where the gels self-aggregate into larger structures with the individual samples oscillating in close proximity to each other.

In the discussion below, our goal is to highlight our observations that the freely moving pieces will undergo autonomous motion in response to self-generated gradients in u. We illustrate this concept through the three cases described below.

5.1 Communication in a row of eight BZ gels

Fig. 11a shows the initial arrangement of eight identically sized BZ cubes that are placed equidistant from each other in a simulation box that is 196 × 41 × 15 units in size. The concentration of activator is maintained at $u = 0$ at the edges of this simulation box and we impose no-flux boundary conditions for u at the top and bottom walls. The side of each cube has a length of $l = 10.5$ units, which corresponds to roughly 0.26 mm (as calculated from the scaling relationships given at the end of Section 4.1) The initial separation between the centers of adjacent cubes is $d = 25$ units and the distance between the outer surface of the gel and the simulation box along the x direction is $d_x = 5$ and along the y direction is $d_y = 15$ units. The gels are numbered sequentially (from left to right). Cubes 1–8 are in the oscillatory state and hence, as the reaction proceeds within the gels, the cubes begin to undergo autonomous pulsations. As the activator u is generated by the BZ reaction and diffuses through the polymer network, it also spreads into the solution between the gels and thus, initiates the interactions between neighboring units.

Fig. 11b shows that the collective net motion within this array of eight motile cubes starts with the outer cubes at the ends of the simulation box in x-direction (*i.e.*, cube 1 on the left and cube 8 on the right); namely, these cubes move away from the edges of the box and towards their respective neighbors. Since cubes 1 and 8 border the walls, they ''sense'' the $u = 0$ condition on their ''outer'' surface (the surface facing the wall) and experience the u generated by the adjacent gel on their ''inner'' surface. As noted above, the oscillation frequency ω increases with increases in u within the solution.[66] Since the concentration of u is higher for the ''inner'' surface of the cube than the outer surface, the inner surface has a higher intrinsic frequency.[66] It is known that in a system containing multiple oscillators, the region with the highest ω determines the ultimate direction of wave propagation.[90,91] Consequently, the chemical wave propagates from the inner to the outer surface of the cube. The net process causes the ''pumping'' of some amount of solvent from the inner space to the outer regions. While this pumping led to the bending of the cilia (see Section 4.2.3), in the case of the freely sliding gels, it leads to the net motion of the BZ cubes, with the gels moving in the direction opposite to the direction of wave propagation.[2,3] Hence, cubes 1 and 8 migrate towards their respective neighbors.

With cubes 1 and 2 (as well as cubes 7 and 8) now lying in closer proximity (see Fig. 11b), any subsequent build up of u will occur between cubes 2 and 3 (and cubes 6 and 7). Just as in Fig. 8c and d, the distribution of u depends markedly on the separation between the gels and the relatively large space between cubes 2 and 3 (and cubes 6 and 7) means that a large fraction of u now remains localized between these separated cubes. As can be seen in Fig. 11c, the high concentration of u at these locations appears to act as a chemo-attractant, with the cubes 1 and 2 moving closer to cube 3 (and similarly, cubes 7 and 8 moving closer to cube 6). Analogous to the examples of the stationary gels, the chemomechanical signal propagates throughout the system. In the motile gels, however, the sensing of this signal results in the remarkable coordinated, directed movement of the pieces.

The image in Fig. 11c again confirms that the gels move along a gradient toward to the highest concentration of u in system. A comparison of Fig. 11c and d reveals that this

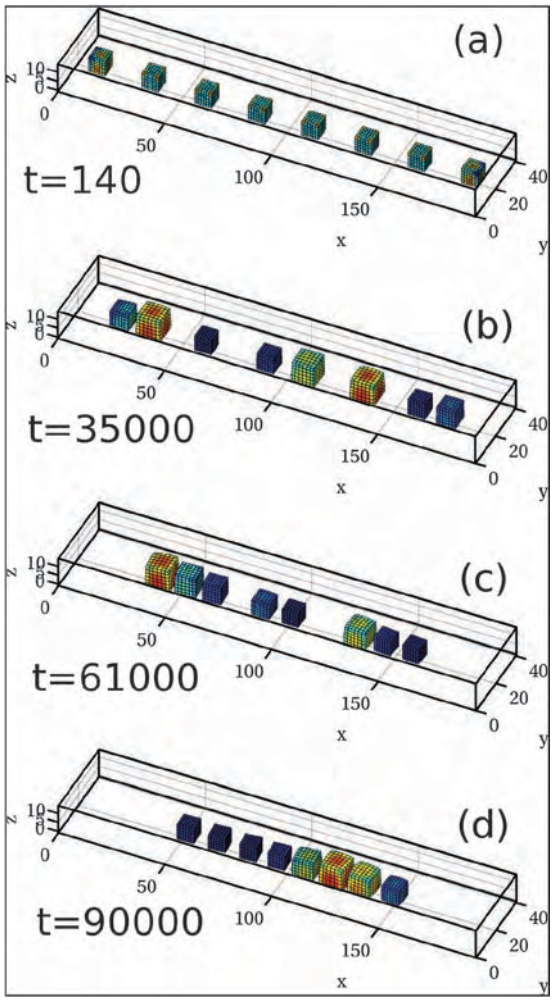

Fig. 11 Self-assembly of self-oscillating BZ-gels. Snapshots of eight cubic BZ gels self-aggregating under the influence of self-generated distribution of u in solution at times t = 140 (a), 35 000 (b), 61 000 (c) and 90 000 (d). The initial size of all the gels is same and is $l_x \times l_y \times l_z$ = 10.5 × 10.5 × 10.5 units and simulation box size is $L_x \times L_y \times L_z$ = 196 × 41 × 15 units. Initial distance between gels' outer surfaces and the simulation box boundary is set equal to 15 and 5 units in x and y-directions respectively.

behavior is repeated at later times, with the gap between cubes 3 and 4, as well as cubes 5 and 6, containing high concentrations of u that draw the cubes closer together. The late time behavior in Fig. 11d shows that all the pieces now lie in close proximity; the final average separation between the gel centers is approximately 14 units. (Note that the excluded volume interactions between the gels affects the final separation between the cubes;[3] here, we used same values for the interaction parameters as given in ref. 3.) As can be seen in Fig. 11, this structural arrangement was accomplished in stages; in each step, the gels moved to the highest concentration of u in the environment. The latter process broadly resembles the auto-chemotactic behavior of the cellular slime mold, which aggregates into large-scale structures in response to chemical signals that they themselves emit.

In the following example, we show that the BZ gels can be made to not only self-assemble into a large structure, but by manipulating the external conditions, these structures can be disassembled. Hence, these gels constitute ideal materials for dynamic reconfiguration and, through specific external stimuli, could be driven reversibly into a variety of different shapes.

5.2 Aggregation and controlled separation of four auto-chemotactic gels

Fig. 12 shows four equally-sized BZ gel cubes that are initially placed in a symmetric square arrangement on the bottom surface of the simulation box; the cubes can slide freely on this substrate. The cubes are the same size as in the example above and the initial distance between the separated cube centers is d = 25 units; hence, the cubes lie relatively far apart (*i.e.*, greater than the linear dimension of the gel). The boundary conditions are the same as noted above, but the simulation box dimensions are now 56 × 56 × 13 units.

Fig. 12b shows the distribution of u for the cubes in Fig. 12a. At this moment of time, the gels are in a relatively collapsed phase and a fraction of u has diffused from the gel into the solution. Given the symmetric arrangement of the cubes and the u = 0 constraint at the box edges, the highest accumulation of u occurs in the region between the four cubes. Due to this spatial distribution of u, the cubes eventually move much closer together, as seen in Fig. 12c and d.

The behavior seen in Fig. 12c and d follows the pattern exhibited in the other examples described here and can be explained as follows. With the concentration of u being higher for the ''inner'' surfaces of the cubes than the outer surfaces, the inner surfaces have a higher intrinsic frequency. Thus, the waves propagate from the inner corners to the outer walls. As noted above, these traveling waves effectively ''push'' the solvent to the outer portions of the box, and due to the inter-diffusion of the polymer and solvent, all the gel cubes are driven to move in the opposite direction.[2,3] In other words, the gel undergoes a net displacement that is opposite in direction to the propagation of the traveling waves[51,52] and, consequently, the cubes migrate towards the center of the simulation box.

At the sufficiently late time shown in Fig. 12d, the cubes have reached the center of the box and will continue to oscillate at this position.[3] A remarkable feature of this system is that the assembled cubes can be driven to dissemble. This behavior can be achieved by altering the distribution of u in the outer solution, so that the concentration of u is higher at the edges of the system than in the center. To illustrate this behavior, we started with the late time scenario shown in Fig. 12d and set u = 0.4 along all the edges of the simulation box (at time $t = 3 \times 10^4$). Fig. 13a shows the gels' positions (at time t = 32 500) within this box shortly after this change. At this moment in time, the concentration of u is highest at the sides of the simulation box (see Fig. 13b). Fig. 13c and d clearly reveal that the cubes effectively disperse from their central location and each cube migrates towards an outer wall.

To quantify this chemotaxing behavior, we calculate the time evolution of the effective area occupied by the entire structure. Specifically, at each moment of time, we calculate the area between the centers of all four cubes as shown

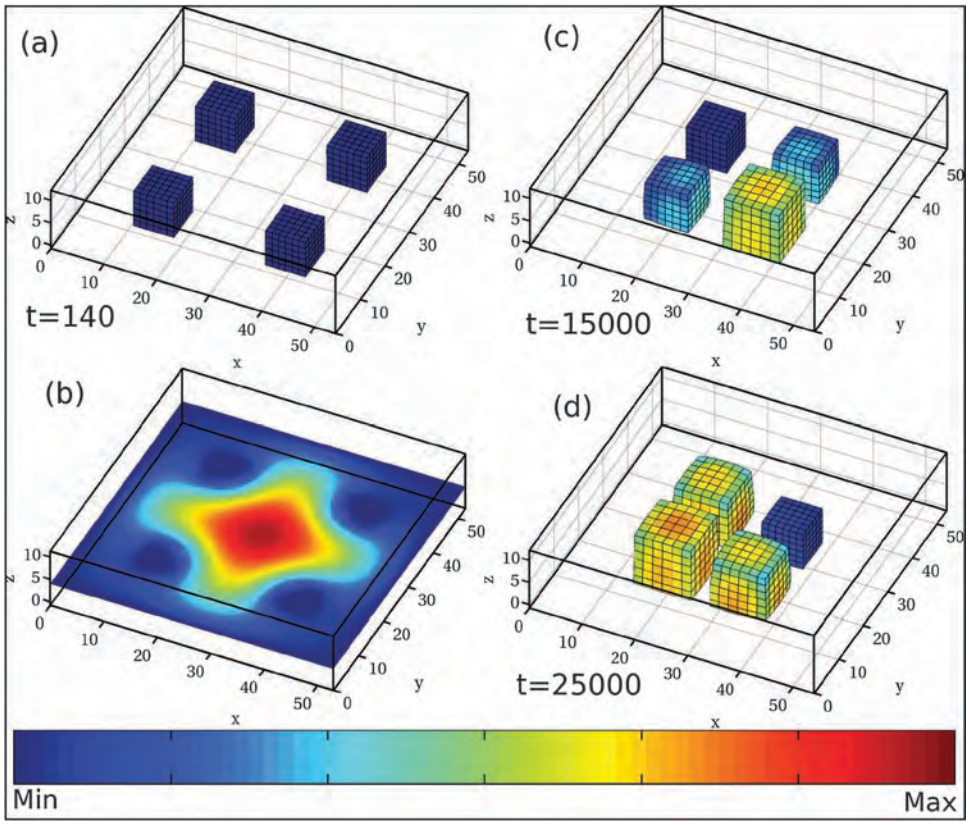

Fig. 12 Snapshots of four cubic BZ gels self-aggregating under the influence of the self-generated distribution of u in solution at times t = 140 (a), 15 000 (c) and 25 000 (d). In (a), (c) and (d), color indicates local concentration of v in the gels and in (b) color indicates distributions of local concentration of u in solution within the horizontal plane (taken at z = 4) at time t = 140. Blue and red color represents respectively the minimum and maximum values of concentrations as shown in the color bar at the bottom of the figure. For v, minimum and maximum values are respectively 0 and 0.4 and that for u are 0 and 0.03. The initial size of all the gels is same and is $l_x \times l_y \times l_z = 10.5 \times 10.5 \times 10.5$ units and simulation box size is $L_x \times L_y \times L_z = 56 \times 56 \times 13$ units. Initial distance between gels' outer surfaces and the simulation box boundary is set equal to 10 units.

schematically at the top of Fig. 14. The blue points in Fig. 14 correspond to the respective images in Fig. 12a, c, and d and the red points correspond to the respective images in Fig. 13a, c, and d. Fig. 14 clearly shows that system not only undergoes autonomous self-assembly, but also disassembly. The nature of these chemotactic interactions is controlled by imposing specific values of u at the boundaries of the system at a given moment in time (at $t = 3 \times 10^4$ for an example in Fig. 14) and the self-generated gradients of u that arise from the periodic redox reaction in the gels. Clearly, other migration patterns of gels can be generated by introducing inhomogeneous boundary conditions, with u being set to distinct minima or maxima on each of the different walls. Such spatial variations in the activator can be used to create a variety of different self-assembled shapes from these autonomously moving, chemo-responsive gels.

5.3 Self-assembly of gels freely suspended in solution

Finally, we consider eight cubes that are suspended in solution, as shown in Fig. 15. In practice, it may be difficult to control the arrangement of these cubes in such a precise manner. Nonetheless, we include this example to show the robustness of the chemo-responsive effect. Fig. 15a shows the initial position of eight cubes that are located near the corners of the simulation box. Again, the boundary condition $u = 0$ is maintained at the edges of this box. Fig. 15b shows the distribution of u at relatively late times, revealing that the highest concentration of the activator is in the center of the box. As can be seen in Fig. 15c, the BZ cubes migrate to this region of highest u concentration. Fig. 15d shows the distance between the center of each cube and the center of the simulation box, $d(t)$, as a function of time, revealing that all the cubes move to this central region. The inset in Fig. 15d shows the trajectories of all eight gels and again highlights the chemotactic motion towards the center of the box.

One could introduce structural heterogeneities into these BZ cubes to control their shapes and to modify their collective motion. In addition, one could exploit the photosensitivity of the cubes and utilize non-uniform illumination to further control their migratory behavior. The studies on the phototaxing BZ worms[3,51,52] indicate that spatially localized light could be used to control the collective motion of multiple motile gels. In effect, one could create a school of BZ "fish" that all move in a specified direction, or could use a single, stimulated gel to create a driving force to collect gels in one location as in bacterial quorum sensing.[94]

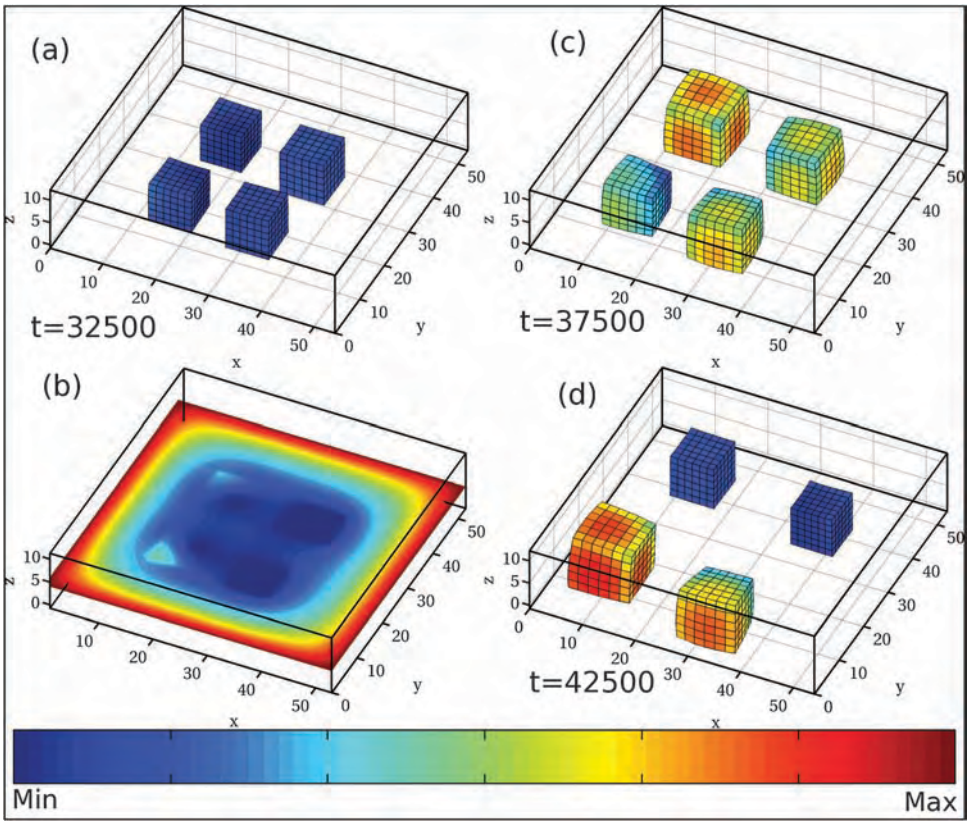

Fig. 13 Snapshots of four cubic BZ gels moving apart from each other towards the outer walls under the influence of high $u = 0.4$ set at all these outer boundaries of the simulation box. All of the simulation parameters are the same as in Fig. 12. Here, we took a late time morphology for the case in Fig. 12 and at $t = 30\,000$ (when all four cubes are aggregated close to the center of the box) set at $u = 0.4$ set at all these outer boundaries of the simulation box. In (a), (c) and (d), color indicates local concentration of v in the gels and in (b) color indicates distributions of local concentration of u in solution within the horizontal plane (taken at $z = 4$) at time $t = 32\,500$. The images correspond to the simulation times $t = 32\,500$ (a and b), 37 500 (c) and 42 500 (d). For both, v and u, minimum and maximum values are set to 0 and 0.4, respectively.

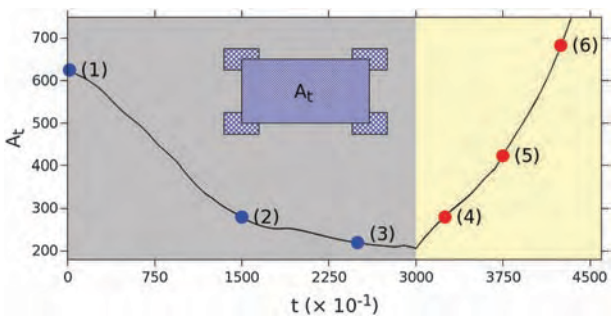

Fig. 14 Time evolution of area A_t covered by four gels (calculated as at each time step t as schematically shown in the inset). Grey region ($0 \leq t \leq 29\,999$) represents the system when $u = 0$ is set at all the solution boundaries in x and y – directions and light yellow region ($30\,000 \leq t \leq 44\,000$) represents the system when $u = 0.4$ is set at all the solution boundaries in x and y – directions. Snapshots of the gels corresponding to times $t = 140$ (1), 15 000 (2), 25 000 (3), 32 500 (4), 37 500 (5) and 42 500 (6) are also shown in Fig. 12(a), (c) and (d) and Fig. 13(a), (c) and (d) respectively.

6. Conclusions

The above examples reveal that self-oscillating gels undergoing the BZ reaction are capable of a distinct biomimetic behavior: the ability to send and receive chemical signals, and to respond to such communication by autonomously performing a concerted action. In effect, these gels are responsive to a stimulus that they themselves generate.

There are number of important implications of this behavior. As indicated by the example involving the mechanically induced oscillations discussed in Section 3, the system can act as a novel pressure sensor.[69] Namely, if one of the gels in the array is mechanically loaded to a sufficient degree, it sends a signal across the entire system. Such a response shares qualitative similarities with biological signaling cascades; for example, such a gel network mimics the transmission of a signal away from the stimulation site in neural networks. Aspects of this behavior also mimic the skin's response to impact; namely, analogous to bruising, the gels temporarily change color in response to loading. Notably, a coating of the BZ gel could act as an artificial skin layer for robotic applications, allowing robots to "sense" pressure and even indicate damage.

The studies on the communicating cilia also yield guidelines for useful technological applications. Specifically the attributes of the BZ cilia could be exploited for a range of microfluidic applications in which, for example, an external light source could be used to direct the movement of a soft "conveyor

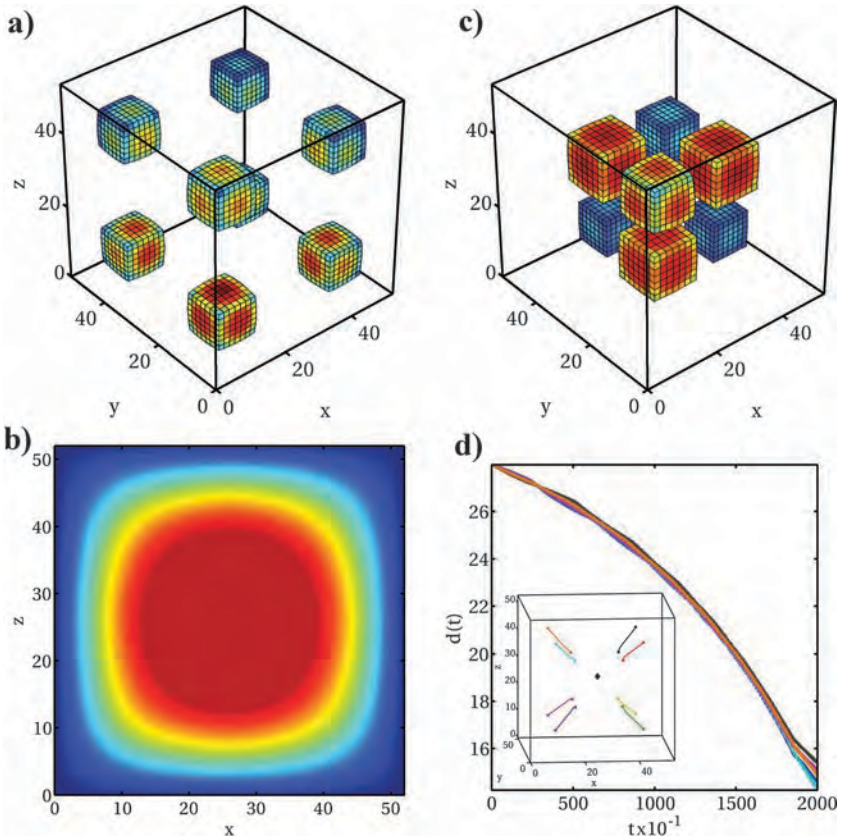

Fig. 15 Simulation of an array of eight interacting BZ gel cubes. Each cube of size 8 × 8 × 8 nodes is placed in the simulation box of size 53 × 53 × 53 at an initial distance of 4.0 from its adjacent boundaries. The inner faces of each gel are initially separated by a distance of 20 from the inner faces of its nearest neighbors. The activator concentration u = 0.0 is maintained at all the fluid boundaries. (a) Initial location of the cubes. (b) Distribution of u in the solution. (c) Later location of the cubes. (d) Distance between the center of each cube and the center of the simulation box as a function of time.

belt''[78,79,93] and thus, manage the transport of microscopic objects within the devices. As indicated above, the motion of the BZ cilia are relatively slow (on the order of 10 μm s^{-1}), and hence, this conveyor belt would be most effective in scenarios that involve diagnostic studies or analyses of the species as they are transported through the microchannels.

We also considered examples of BZ gels that could move freely on a surface. The ability of these systems to undergo directed autonomous motion in response to the self-generated signals has broad implications in the design of adaptive materials. The example involving the array of eight mobile pieces indicates that BZ gels can undergo a form of ''self-recombining''. Consider a longer rectangular sample that is cut into eight cubes and these cubes are placed relatively far apart to create the array shown in Fig. 11. Then the auto-chemotactic behavior within this system drives the cut pieces to move autonomously and recombine into a structure resembling the original, uncut sample. In this sense, these gels demonstrate a primitive form of materials' regeneration; while the severed pieces are not re-grown *de novo*, the self-directed, self-sustained motion of the gels nonetheless leads to an effective recovery of the sample's original shape.

We note that the above findings constitute a vital step toward designing the next generation of self-healing materials. Currently, severed pieces of self-healing gels or networks can only form bonds when these pieces are brought together by an external agent (*e.g.*, placed in contact *via* human intervention).[95–98] To the best of our knowledge, there is no example of synthetic materials that bring themselves together as the first step in the self-healing process. Notably, the sides of the isolated BZ gels can potentially be functionalized with reactive groups that would promote bond formation as the separate pieces come within a critical distance of each other. Hence, these auto-chemotactic materials could pave the way for designing severed materials that autonomously come together and then form strong bonds that bind the units and thereby, restore the mechanical properties of the system, to yield a truly self-healing material.

Finally, we showed that by introducing high concentrations of u at the outer boundaries of the system, the assembled structures can be ''disassembled'' since the pieces would migrate to the high u at these edges. In previous studies, we showed that the motion of the BZ gels can be guided by light to follow specific paths.[3,51,52] The latter studies indicate that the separated units shown in Fig. 11–14 could be guided by light to self-organize into a completely different morphology. In this sense, the BZ gels resemble pieces of a construction toy that can be reused to build multiple structures and thus, provide a new route for creating dynamically reconfigurable materials.

Acknowledgements

ACB gratefully acknowledges financial support from ARO (for partial support of V. V. Yashin), the AFOSR (for partial support of O. Kuksenok), and the ONR (for partial support of A. Bhattacharya). KJVV and ACB gratefully acknowledge support from the NSF MRSEC CMSE (for support of I. C. Chen and partial support of P. Dayal, and D. Deb).

References

1 J. S. King and R. H. Insall, *Trends Cell Biol.*, 2009, **19**, 523–530.
2 I. R. Epstein, V. K. Vanag, A. C. Balazs, O. Kuksenok, P. Dayal and A. Bhattacharya, *Acc. Chem. Res.*, 2012, **45**, 2160–2168.
3 P. Dayal, O. Kuksenok and A. C. Balazs, *Proc. Natl. Acad. Sci. U. S. A.*, 2013, **110**, 431–436.
4 R. Yoshida, T. Takahashi, T. Yamaguchi and H. Ichijo, *J. Am. Chem. Soc.*, 1996, **118**, 5134–5135.
5 R. Yoshida, S. Onodera, T. Yamaguchi and E. Kokufuta, *J. Phys. Chem. A*, 1999, **103**, 8573–8578.
6 B. P. Belousov, *Collection of Short Papers on Radiation Medicine*, Medgiz, Moskow, 1959.
7 A. N. Zaikin and A. M. Zhabotinsky, *Nature*, 1970, 535–537.
8 R. Yoshida, E. Kokufuta and T. Yamaguchi, *Chaos*, 1999, **9**, 260–266.
9 R. Yoshida, *Adv. Mater.*, 2010, **22**, 3463–3483.
10 V. Labrot, P. De Kepper, J. Boissonade, I. Szalai and F. Gauffre, *J. Phys. Chem. B*, 2005, **109**, 21476–21480.
11 T. G. Szanto and G. Rabai, *J. Phys. Chem. A*, 2005, **109**, 5398–5402.
12 A. J. Ryan, C. J. Crook, A. Smith and R. A. L. Jones, *Phys. Chem. Chem. Phys.*, 2002, **4**, 1367–1369.
13 A. J. Ryan, C. J. Crook, J. R. Howse, P. Topham, R. A. L. Jones, M. Geoghegan, A. J. Parnell, L. Ruiz-Perez, S. J. Martin, A. Cadby, A. Menelle, J. R. P. Webster, A. J. Gleeson and W. Bras, *Faraday Discuss.*, 2005, **128**, 55–74.
14 P. Borckmans, K. Benyaich and G. Dewel, *Int. J. Quantum Chem.*, 2004, **98**, 239–247.
15 J. C. Leroux and R. A. Siegel, *Chaos*, 1999, **9**, 267–275.
16 R. A. Siegel, in *Chemomechanical Instabilities in Responsive Materials*, ed. P. Borckmans, d. P. Kepper, A. R. Khokhlov and S. Métens, Springer, Dordrecht, The Netherlands, 2009, p. 273.
17 X. M. He, M. Aizenberg, O. Kuksenok, L. D. Zarzar, A. Shastri, A. C. Balazs and J. Aizenberg, *Nature*, 2012, **487**, 214–218.
18 S. Sasaki, S. Koga, R. Yoshida and T. Yamaguchi, *Langmuir*, 2003, **19**, 5595–5600.
19 K. Miyakawa, F. Sakamoto, R. Yoshida, E. Kokufuta and T. Yamaguchi, *Phys. Rev. E: Stat. Phys., Plasmas, Fluids, Relat. Interdiscip. Top.*, 2000, **62**, 793–798.
20 I. C. Chen, O. Kuksenok, V. V. Yashin, R. M. Moslin, A. C. Balazs and K. J. Van Vliet, *Soft Matter*, 2011, **7**, 3141–3146.
21 Y. Zhang, N. Li, J. Delgado, N. Zhou, R. Yoshida, S. Fraden, I. R. Epstein and B. Xu, *Soft Matter*, 2012, **8**, 7056–7061.
22 M. L. Smith, K. Heitfeld, C. Slone and R. A. Vaia, *Chem. Mater.*, 2012, **24**, 3074–3080.
23 I. Y. Konotop, I. R. Nasimova, N. G. Rambidi and A. R. Khokhlov, *Polym. Sci., Ser. B*, 2011, **53**, 26–30.
24 I. Y. Konotop, I. R. Nasimova, N. G. Rambidi and A. R. Khokhlov, *Polym. Sci., Ser. B*, 2009, **51**, 383–388.
25 P. Yuan, O. Kuksenok, D. E. Gross, A. C. Balazs, J. S. Moore and R. G. Nuzzo, *Soft Matter*, 2013, **9**, 1231–1243.
26 S. Maeda, Y. Hara, T. Sakai, R. Yoshida and S. Hashimoto, *Adv. Mater.*, 2007, **19**, 3480–3484.
27 Y. Shiraki and R. Yoshida, *Angew. Chem., Int. Ed.*, 2012, **51**, 6112–6116.
28 S. J. Ebbens and J. R. Howse, *Soft Matter*, 2010, **6**, 726–738.
29 A. Sen, M. Ibele, Y. Hong and D. Velegol, *Faraday Discuss.*, 2009, **143**, 15–27.
30 G. V. Kolmakov, V. V. Yashin, S. P. Levitan and A. C. Balazs, *Proc. Natl. Acad. Sci. U. S. A.*, 2010, **107**, 12417–12422.
31 M. M. Caruso, D. A. Davis, Q. Shen, S. A. Odom, N. R. Sottos, S. R. White and J. S. Moore, *Chem. Rev.*, 2009, **109**, 5755–5798.
32 S. C. Olugebefola, A. M. Aragon, C. J. Hansen, A. R. Hamilton, B. D. Kozola, W. Wu, P. H. Geubelle, J. A. Lewis, N. R. Sottos and S. R. White, *J. Compos. Mater.*, 2010, **44**, 2587–2603.
33 R. F. Shepherd, F. Ilievski, W. Choi, S. A. Morin, A. A. Stokes, A. D. Mazzeo, X. Chen, M. Wang and G. M. Whitesides, *Proc. Natl. Acad. Sci. U. S. A.*, 2011, **108**, 20400–20403.
34 T. Yamaguchi, L. Kuhnert, Z. Nagy-Ungvarai, S. C. Mueller and B. Hess, *J. Phys. Chem.*, 1991, **95**, 5831–5837.
35 T. L. Hill, *An Introduction to Statistical Thermodynamics*, Addison-Wesley, Reading, MA, 1960.
36 M. Shibayama and T. Tanaka, *Adv. Polym. Sci.*, 1993, **109**, 1–62.
37 R. Yoshida, *Curr. Org. Chem.*, 2005, **9**, 1617–1641.
38 R. Yoshida, M. Tanaka, S. Onodera, T. Yamaguchi and E. Kokufuta, *J. Phys. Chem. A*, 2000, **104**, 7549–7555.
39 T. Sakai and R. Yoshida, *Langmuir*, 2004, **20**, 1036–1038.
40 R. Yoshida, *Bull. Chem. Soc. Jpn.*, 2008, **81**, 676–688.
41 R. J. Field, R. M. Noyes and E. Koros, *J. Am. Chem. Soc.*, 1972, **94**, 8649–8664.
42 R. J. Field and R. M. Noyes, *J. Chem. Phys.*, 1974, **60**, 1877–1884.
43 S. K. Scott, *Oscillations, Waves, and Chaos in Chemical Kinetics*, Oxford University Press, New York, 1994.
44 A. S. Mikhailov and K. Showalter, *Phys. Rep.*, 2006, **425**, 79–194.
45 J. J. Tyson and P. C. Fife, *J. Chem. Phys.*, 1980, **73**, 2224–2237.
46 J. J. Tyson, in *Oscillations and Traveling Waves in Chemical Systems*, ed. R. J. Field and M. Burger, Wiley, New York, 1985, pp. 93–144.
47 V. V. Yashin and A. C. Balazs, *Macromolecules*, 2006, **39**, 2024–2026.
48 V. V. Yashin and A. C. Balazs, *J. Chem. Phys.*, 2007, **126**, 124707.
49 O. Kuksenok, V. V. Yashin and A. C. Balazs, *Phys. Rev. E: Stat. Nonlinear Soft Matter Phys.*, 2008, **78**, 041406.

50 V. V. Yashin, O. Kuksenok, P. Dayal and A. C. Balazs, *Rep. Prog. Phys.*, 2012, **75**, 066601.
51 P. Dayal, O. Kuksenok and A. C. Balazs, *Langmuir*, 2009, **25**, 4298–4301.
52 P. Dayal, O. Kuksenok and A. C. Balazs, *Soft Matter*, 2010, **6**, 768–773.
53 O. Kuksenok, V. V. Yashin, M. Kinoshita, T. Sakai, R. Yoshida and A. C. Balazs, *J. Mater. Chem.*, 2011, **21**, 8360–8371.
54 V. V. Yashin, S. Suzuki, R. Yoshida and A. C. Balazs, *J. Mater. Chem.*, 2012, **22**, 13625–13636.
55 V. V. Yashin and A. C. Balazs, *Science*, 2006, **314**, 798–801.
56 V. V. Yashin, O. Kuksenok and A. C. Balazs, *Prog. Polym. Sci.*, 2010, **35**, 155–173.
57 H. J. Krug, L. Pohlmann and L. Kuhnert, *J. Phys. Chem.*, 1990, **94**, 4862–4866.
58 O. Steinbock, V. Zykov and S. C. Muller, *Nature*, 1993, **366**, 322–324.
59 V. S. Zykov, O. Steinbock and S. C. Muller, *Chaos*, 1994, **4**, 509–518.
60 V. S. Zykov, G. Bordiougov, H. Brandtstadter, I. Gerdes and H. Engel, *Phys. Rev. Lett.*, 2004, **92**, 018304.
61 B. Costello, A. Adamatzky, I. Jahan and L. A. Zhang, *Chem. Phys.*, 2011, **381**, 88–99.
62 S. Shinohara, T. Seki, T. Sakai, R. Yoshida and Y. Takeoka, *Angew. Chem., Int. Ed.*, 2008, **47**, 9039–9043.
63 B. Barriere and L. Leibler, *J. Polym. Sci., Part B: Polym. Phys.*, 2003, **41**, 166–182.
64 To account for the hydrodynamic effects in gels, the condition of $v = 0$ should be lifted and, correspondingly, the above system of equations should be complemented with the respective Navier–Stokes equation.
65 V. V. Yashin and A. C. Balazs, *Phys. Rev. E: Stat. Nonlinear Soft Matter Phys.*, 2008, **77**, 046210.
66 P. Dayal, O. Kuksenok, A. Bhattacharya and A. C. Balazs, *J. Mater. Chem.*, 2012, **22**, 241–250.
67 F. Sakamoto and K. Miyakawa, *J. Phys. Soc. Jpn.*, 2003, **72**, 2173–2176.
68 S. Tateyama, Y. Shibuta and R. Yoshida, *J. Phys. Chem. B*, 2008, **112**, 1777–1782.
69 I. C. Chen, O. Kuksenok, V. V. Yashin, A. C. Balazs and K. J. Van Vliet, *Adv. Funct. Mater.*, 2012, **22**, 2535–2541.
70 O. Tabata, H. Hirasawa, S. Aoki, R. Yoshida and E. Kokufuta, *Sens. Actuators, A*, 2002, **95**, 234–238.
71 O. Tabata, H. Kojima, T. Kasatani, Y. Isono, R. Yoshida, S. Aoki and R. Yoshida, *IEEE 16th Annual Intl. Conf. Micro Electro Mechanical Syst. (MEMS2003) Proc., IEEE*, 2003, **03**, 12–15.
72 O. Steinbock, P. Kettunen and K. Showalter, *Science*, 1995, **269**, 1857–1860.
73 K. Suzuki, T. Yoshinobu and H. Iwasaki, *Jpn. J. Appl. Phys., Part 2*, 1999, **38**, L345–L348.
74 O. U. Kheowan, E. Mihaliuk, B. Blasius, I. Sendina-Nadal and K. Showalter, *Phys. Rev. Lett.*, 2007, **98**, 074101.
75 M. Toiya, H. O. Gonzalez-Ochoa, V. K. Vanag, S. Fraden and I. R. Epstein, *J. Phys. Chem. Lett.*, 2010, **1**, 1241–1246.
76 J. Delgado, N. Li, M. Leda, H. O. Gonzalez-Ochoa, S. Fraden and I. R. Epstein, *Soft Matter*, 2011, **7**, 3155–3167.
77 M. R. Tinsley, S. Nkomo and K. Showalter, *Nat. Phys.*, 2012, **8**, 662–665.
78 Y. Murase, S. Maeda, S. Hashimoto and R. Yoshida, *Langmuir*, 2009, **25**, 483–489.
79 Y. Murase, M. Hidaka and R. Yoshida, *Sens. Actuators, B*, 2010, **149**, 272–283.
80 A. P. Munuzuri, C. Innocenti, J. M. Flesselles, J. M. Gilli, K. I. Agladze and V. I. Krinsky, *Phys. Rev. E: Stat. Nonlinear Soft Matter Phys.*, 1994, **50**, R667–R670.
81 K. Suzuki, T. Yoshinobu and H. Iwasaki, *Chem. Phys. Lett.*, 2001, **349**, 437–441.
82 O. Kuksenok, V. V. Yashin and A. C. Balazs, *Soft Matter*, 2007, **3**, 1138–1144.
83 O. Kuksenok, V. V. Yashin and A. C. Balazs, *Soft Matter*, 2009, **5**, 1835–1839.
84 B. Huo, X. L. Lu, K. D. Costa, Q. B. Xu and X. E. Guo, *Cell Calcium*, 2010, **47**, 234–241.
85 R. Aihara and K. Yoshikawa, *J. Phys. Chem. A*, 2001, **105**, 8445–8448.
86 A. Bhattacharya and A. C. Balazs, *J. Mater. Chem.*, 2010, **20**, 10384–10396.
87 S. Hirotsu, *J. Chem. Phys.*, 1991, **94**, 3949–3957.
88 R. Yoshida, G. Otoshi, T. Yamaguchi and E. Kokufuta, *J. Phys. Chem. A*, 2001, **105**, 3667–3672.
89 O. Kuksenok, V. V. Yashin and A. C. Balazs, *Phys. Rev. E: Stat. Nonlinear Soft Matter Phys.*, 2009, **80**, 056208.
90 A. S. Mikhailov and A. Engel, *Phys. Lett. A*, 1986, **117**, 257–260.
91 O. U. Kheowan, E. Mihaliuk, B. Blasius, I. Sendina-Nadal and K. Showalter, *Phys. Rev. Lett.*, 2007, **98**, 074101.
92 P. Dayal, O. Kuksenok and A. C. Balazs, *Soft Matter*, 2009, **5**, 5042.
93 R. Yoshida, T. Sakai, Y. Hara, S. Maeda, S. Hashimoto, D. Suzuki and Y. Murase, *J. Controlled Release*, 2009, **140**, 186–193.
94 M. B. Miller and B. L. Bassler, *Annu. Rev. Microbiol.*, 2001, **55**, 165–199.
95 A. Phadke, C. Zhang, B. Arman, C. C. Hsu, R. A. Mashelkar, A. K. Lele, M. J. Tauber, G. Arya and S. Varghese, *Proc. Natl. Acad. Sci. U. S. A.*, 2012, **109**, 4383–4388.
96 K. Imato, M. Nishihara, T. Kanehara, Y. Amamoto, A. Takahara and H. Otsuka, *Angew. Chem., Int. Ed.*, 2012, **51**, 1138–1142.
97 Y. Amamoto, J. Kamada, H. Otsuka, A. Takahara and K. Matyjaszewski, *Angew. Chem., Int. Ed.*, 2011, 1660–1663.
98 M. Nakahata, Y. Takashima, H. Yamaguchi and A. Harada, *Nat. Commun.*, 2011, **2**, 511.